



HHS Public Access

Author manuscript

Adv Mater. Author manuscript; available in PMC 2021 June 01.

Published in final edited form as:

Adv Mater. 2020 June ; 32(25): e2000660. doi:10.1002/adma.202000660.

Phase-Change Materials for Controlled Release and Related Applications

Jichuan Qiu[†],

The Wallace H. Coulter Department of Biomedical Engineering, Georgia Institute of Technology and Emory University, Atlanta, GA 30332, USA

Da Huo[†],

The Wallace H. Coulter Department of Biomedical Engineering, Georgia Institute of Technology and Emory University, Atlanta, GA 30332, USA

Yunan Xia

The Wallace H. Coulter Department of Biomedical Engineering, Georgia Institute of Technology and Emory University, Atlanta, GA 30332, USA

School of Chemistry and Biochemistry, Georgia Institute of Technology, Atlanta, GA 30332, USA

Abstract

Phase-change materials (PCMs) have emerged as a novel class of thermo-responsive materials for controlled release, where the payloads encapsulated in a solid matrix will only be released upon melting the PCM to trigger a solid-to-liquid phase transition. In this Progress Report, we highlight the advances over the past ten years in utilizing PCMs as a versatile platform for the encapsulation and release of various types of therapeutic agents and biological effectors. We begin with a brief introduction to PCMs in the context of desired properties for controlled release and related applications. Among various types of PCMs, we specifically focus on fatty acids and fatty alcohols for their natural availability, low toxicity, biodegradability, diversity, high abundance, and low cost. We then discuss various methods capable of processing PCMs, and their mixtures with payloads, into stable suspensions of colloidal particles, and the different means for triggering the solid-to-liquid phase transition. Finally, we showcase a range of applications enabled by the controlled release system based on PCMs, together with some perspectives on future directions.

Keywords

phase-change material; fatty acid; controlled release; stimuli-responsive; drug delivery

yunan.xia@bme.gatech.edu.

[†]These authors contribute equally to the preparation of this article.

Conflict of Interest

The authors declare no conflict of interest.

1. Introduction

Controlled release has been a main theme of research in biomedicine since the 1960s.^[1,2] Many types of controlled release systems have been developed for dosing therapeutic agents and biological effectors in a manageable manner, enabling a wide variety of applications ranging from disease diagnosis and treatment to tissue engineering.^[2-4] Among various systems, those based on stimuli-responsive materials are particularly attractive owing to their ability to trigger the release and then tightly manage the profile.^[4-7] These materials can serve as carriers for various types of payloads and protect them from pre-release or deactivation during circulation. Upon arrival at the targeted site, the payloads will be unloaded in a controlled manner under the exertion of an external or internal stimulus. The stimuli may include temperature, pH, ultrasound, light, mechanical stress, and/or reactive biomolecules.^[4,5] The on-demand release of drugs with a precise control over the dosage, as well as spatial and temporal resolutions, offers immediate advantages in improving their therapeutic efficacy while reducing the off-target toxicity.

Generally, stimuli-responsive materials should have the following features in order to find use in clinical translation: *i*) gating ability to reduce the off-target toxicity by avoiding pre-release of the payloads without being triggered by a stimulus; *ii*) swift and reversible response to a specific stimulus to allow for repeatedly turning on and off the release; *iii*) feasibility to load multiple types of payloads in high loading capacities; *iv*) biocompatibility and biodegradability to ensure that the carrier materials have no toxicity and can be degraded or cleared from the body after the use; and *v*) easy to obtain and engineer. On this basis, polymeric materials capable of responding to specific stimuli have been extensively explored for controlled release.^[3,7,8] However, the complicated preparation procedures, as well as the low degradability and high toxicity of some polymers place a major limitation on their translational capability. On the other hand, phase-change materials (PCMs) based on fatty acids and their derivatives offer a simple and effective platform for controlled release owing to their precise responses to the variations in temperature.^[9-11] The release is controlled by leveraging the change in molecular mobility for a PCM during its solid-to-liquid phase transition. Upon melting, the payloads trapped in the solid matrix of a PCM will be swiftly released with the melted PCM.

In this Progress Report, we summarize the advances over the past decade in exploring PCMs as thermo-responsive materials for controlled release and related applications. We begin with an introduction to PCMs and their desired properties. We specially focus on PCMs made of natural fatty acids and fatty alcohols, together with a brief discussion about their biological features. We then focus on methods developed for the preparation of PCMs as stable dispersions of micro- and nanoscale particles. We pay particular attention to the cases where PCMs serve as a smart filling for hollow particles. We also discuss methods suitable for triggering the phase transition of a PCM. Afterwards, we highlight the use of PCMs for controlled release of functional materials, including various types of therapeutic small molecules, bioactive macromolecules, and nanoparticles, with potential applications in various biomedical fields. At the end, we summarize the pros and cons of a PCM-based controlled release system and offer some perspective on the future development.

2. Phase-Change Materials

2.1. Desired Properties

Traditionally, PCM refers to a certain type of substance featuring a great latent heat of fusion with regards to melting or solidifying at a nearly constant temperature.^[9] In the process of phase transition, PCM is able to store and release a large amount of heat within a relatively narrow range of temperature variation (Figure 1A). For example, relative to the conventional thermal storage materials such as water or rocks, an equivalent volume of PCM can store or release 5–14 times more heat.^[12] To this end, PCMs have been widely explored for use as thermal materials for heat management.^[13–15] It should be pointed out that the storage or release of energy is only one reflection of the changes in intermolecular interactions (*e.g.*, van der Waals forces and hydrogen bonding) in PCM during phase transition.^[9] The change in intermolecular interactions also causes drastic variations in other physicochemical parameters such as mobility and density. For example, when butter is melted upon heating in a pan, its mobility will be increased substantially to allow flow (Figure 1B). The increase in mobility during a solid-to-liquid transition can be leveraged to control the release of payloads trapped in a solid matrix, leading to a temperature-responsive release system. Benefiting from the changes in physicochemical properties during the phase transition, PCMs have also been explored as functional materials for other applications such as information storage, detection, and barcoding.^[16–18]

2.2. Fatty Acids and Fatty Alcohols

Although nearly all substances can undergo a solid-to-liquid phase transition, only a small number of them can be applied to controlled release *in vivo* and related biomedical applications considering the phase transition temperature and biosafety. For example, some organic compounds such as paraffin C₂₃ (with a melting point at 47.5 °C), as well as some inorganic salts such as Ca(NO₃)₂·4H₂O (with a melting point at 47 °C), can be melted slightly above our body temperature (37 °C).^[15,19] However, their translation into practical use has never been achieved because of the biosafety concern and/or engineering difficulties. In comparison, natural fatty acids show a more promising future owing to their natural availability, low toxicity, biodegradability, diversity, abundance, and low cost.^[20–23] A fatty acid is a carboxylic acid comprised of a long aliphatic chain, either saturated or unsaturated. Most natural fatty acids have an unbranched chain with an even number of carbon atoms ranging from 4–28. Table 1 shows a list of them with melting points in the range of 20–80 °C. They naturally exist in the form of triglycerides, phospholipids, and cholesteryl esters in animal or vegetable fats, and are critical structural components of cells and important dietary source of energy for animals.^[24] Upon circulation in blood and entry into cells, the fatty acid will be broken down through a catabolic process known as β -oxidation, which is mainly executed in mitochondria.^[25,26] Natural fatty acids have been used as biocompatible and biodegradable drug carriers as early as in the 1990s, albeit no attention was paid to their properties related to phase transition at that time.^[22,23] The amphiphilic nature of fatty acids owing to the non-polar aliphatic chain and the polar carboxylic acid head group makes them compatible to both hydrophobic and hydrophilic payloads. It was not until 2010 when lauric acid (with a melting point at 44 °C) was first reported as a PCM for temperature-controlled release of biomacromolecules.^[11]

Fatty alcohols have a structure similar to that of fatty acids, and they are typically straight-chain primary alcohols. They naturally exist in vegetable oil and animal fat. Fatty alcohols with a chain length of up to C₁₈ are known to be biodegradable.^[9] To this end, fatty alcohols have also been considered as candidates for controlled release of drugs. Same as fatty acids, the melting points of fatty alcohols generally have a positive correlation with the number of carbon atoms in the chain (Table 1). Among various fatty alcohols, 1-tetradecanol, with a melting point at 38 °C, was the first to be applied as a PCM for temperature-controlled release of dextran.^[11] Since its phase transition takes place at a temperature slightly above 37 °C, it only needs a small amount of energy to trigger the release of payloads. Considering their great potential in future translations, here we mainly focus on PCMs based on fatty acids and fatty alcohols.

2.3. Eutectic Mixture of Fatty Acids

Although natural fatty acids are a good choice for controlled release owing to their excellent biocompatibility, it is difficult to obtain a PCM made of a pure fatty acid with a melting point close to the physiological temperature (37 °C) of human body (Table 1). In addition, a single fatty acid tends to form a highly crystalline structure during solidification, forcing the payloads to be phase-separated from the fatty acid matrix and thus lowering the encapsulation capacity of the drugs and causing undesired burst release.^[22,23,27] To address these challenges, a eutectic mixture of two or even more fatty acids, with a melting point lower than those of all the constituents, is proposed as a replacement for the single-component fatty acid in achieving the desired melting points while altering the crystallization behavior of the fatty acids to increase the drug loading capacity.^[21,28,29] In one example, lauric acid (with a melting point at 44 °C) and stearic acid (with a melting point at 69 °C) are mixed at a weight ratio of 4:1 to obtain a eutectic mixture exhibiting a single solid-liquid phase transition at 39 °C.^[28] Significantly, the phase transition of such a eutectic mixture can be triggered more easily under heating when compared with either lauric acid or stearic acid.

3. Processing PCMs into Colloidal Particles

3.1. Emulsification under Shear or in a Fluidic Device

In applying PCMs to biomedical research, it is critical to process them into colloidal particles with uniform sizes while containing theranostic agents. Emulsification under a shear force is the most straightforward and effective way to obtain PCM colloidal particles. In a typical process, the PCM, in the form of solution or melt, is dispersed in an anti-solvent (generally, water) containing an appropriate emulsifier and then broken into micro- or nanoscale droplets through mechanical stirring or sonication (Figure 2A).^[30,31] Upon either cooling or solvent evaporation, PCM colloidal particles are obtained. In this approach, the theranostic agents can be introduced into the particles by simply dissolving them in the PCM solution or melt. The size of the resultant PCM particles is strongly dependent on the mechanical force involved and such a force tends to be heterogeneously distributed across the system, leading to the formation of polydispersed particles.^[32] For this method, the poor uniformity in size distribution is an inevitable problem, even though it has shown great success in the preparation of PCM colloidal particles on a relatively large scale.^[30,31]

The uniformity issue can be addressed by achieving emulsification under a viscous drag force at the tip of the inner capillary of a fluidic device for the generation of uniform droplets one at a time.^[32,33] Another major advantage of the fluidic system is its capability to independently vary the size, structure, and composition of the resultant particles.^[32,34–36] Figure 2B shows a schematic drawing of a typical tubular fluidic device capable of generating uniform PCM particles.^[37] The device consists of two concentric capillaries. In a typical process, the PCM, in the form of solution or melt, and an aqueous solution containing an emulsifier are injected into the inner and outer capillaries, respectively, through the use of syringe pumps. At appropriate flow rates for both fluids, individual PCM droplets are continuously formed at the tip of the inner capillary due to the collective effect of viscous drag force and surface tension.^[38] Upon solvent evaporation or cooling, the droplets are converted into solid PCM particles. For this method, one can tune the size of the PCM particles by changing the flow rates of the inner and/or outer fluids. Figure 2C shows an optical micrograph of n-octadecane droplets produced using a fluidic device. The particles had an average diameter of 360 μm and were stabilized by polyurea. Figure 2D shows a scanning electron microscopy (SEM) image of the PCM particles obtained by freeze-drying the droplets.

3.2. Electrospaying

Electrospaying, which shares the same mechanism as electrospinning, has been extensively used for the preparation of micro- and nanoscale particles with various compositions and structures due to its simplicity and low cost.^[39–41] The setup typically comprises of a high-voltage power supply, a syringe pump, and a spinneret. When a fluid is pumped out through the spinneret, it tends to form a hemispherical droplet due to the confinement of surface tension. When connected to a high-voltage power supplier, the surface of the droplet will be covered by charges of the same sign, forcing the droplet to break into much smaller droplets due to electrostatic repulsion.^[40,42] Upon solvent evaporation, solid particles will be obtained. Using this technique, PCM particles were obtained by electrospaying an n-propanol solution containing 4.5% stearic acid and 0.5% ethyl cellulose.^[43] Payloads could be readily loaded into the matrix of the particles by co-dissolving them with stearic acid in the solution. Alternatively, the payloads could be loaded as a core inside a shell made of a PCM through the use of a coaxial electrospaying setup.^[44,45] In a typical process, the eutectic mixture of lauric and stearic acids was dissolved in a mixture of ethanol and dichloromethane and used as the outer solution, while payloads dissolved in an aqueous gelatin solution was supplied as the inner solution.^[44] When pumping these two solutions through a coaxial spinneret, PCM particles containing the payloads in the core were obtained.

3.3. Anti-Solvent Precipitation

Anti-solvent precipitation is another simple method for producing PCM colloidal particles, especially for those with sizes on the nanoscale.^[23,27] Generally, this method requires two solvents that are miscible with each other. In a typical process, the PCM is firstly dissolved in a solvent phase (*e.g.* ethanol), followed by dropwise adding them into the anti-solvent phase (*e.g.* water) containing an appropriate stabilizer under mechanical stirring. The PCM will precipitate out and aggregate into nanoparticles because of their poor solubility in the

anti-solvent phase.^[28] The anti-solvent-induced precipitation can also be achieved in a fluidic device for precisely controlling the mixing of the two phases. In a recent study, our group applied such a fluidic device to continuous production of PCM nanoparticles with a uniform size distribution.^[46] The device is illustrated in Figure 3A. In a typical process, an ethanol solution of PCM (*e.g.*, the eutectic mixture of lauric and stearic acids) and another aqueous solution of phospholipids were injected into the concentric capillaries to serve as the focused and focusing phases, respectively. The phospholipids were added due to their ability to encapsulate and stabilize the resultant PCM nanoparticles.^[28,47,48] As the ethanol solution (solvent phase) met with the aqueous solution (anti-solvent phase) at the tip of the capillary, the PCM was forced to precipitate out as nanoparticles at the interface of the flow. Figure 3B shows a TEM image of the as-obtained PCM nanoparticles with an average diameter of 53 nm.^[46] Furthermore, uniform PCM nanoparticles with sizes ranging from 10 to 100 nm could be routinely obtained by adjusting the ratio of flow rates between the two phases and the concentration of PCM (Figure 3C). It should be pointed out that therapeutic agents, near infrared (NIR) dyes, and even nanoparticles, could all be readily loaded in the PCM nanoparticles by dissolving or dispersing them in the PCM solution.^[28,46,49,50]

4. Stabilization of PCM Colloidal Particles

In applying PCMs to nanomedicine, it is pivotal to process them as stable colloidal particles in an aqueous medium under the physiological condition. Unfortunately, colloidal particles made of fatty acids or fatty alcohols are inherently susceptible to agglomeration in an aqueous medium due to the hydrophobicity associated with the long aliphatic chain.^[23] The particles tend to aggregate into larger structures and then float on the surface of an aqueous medium. When PCM nanoparticles are used for energy storage, their surface can be coated with a solid shell made of silica or polystyrene (PS) to enhance their colloidal stability.^[30,51–53] However, this method will cause complication to the drug delivery system because the solid shell will make it difficult for the payloads to pass through. Alternatively, soft shells made of amphiphilic molecules such as phospholipids have been developed to stabilize PCM colloidal particles.^[28,46] In addition, PCMs can be encapsulated in well-defined hollow and porous nanoparticles, such as those made of SiO₂ and Au, to obtain stable colloidal suspensions.^[54–56] A combination of such capsules with PCM also improves the loading capacity of payloads while preventing them from pre-leakage. Furthermore, functional groups such as targeting moieties can be readily added to the surface of the hollow capsules to enable site-specific drug delivery.^[57,58] Table 2 shows a brief summary of the strategies effective in stabilizing PCM colloidal particles and their associated advantages and disadvantages in terms of loading and release of the payloads.

4.1. Covering the Surface with a Monolayer of Phospholipids

Phospholipids are the main components of cellular membranes. They have an amphiphilic structure, together with superb biocompatibility *in vivo*. When introduced into an aqueous medium, they can assemble into various types of supramolecular structures in an effort to minimize the exposure of their hydrophobic chains to water. Leveraging this attribute, PCM nanoparticles have been obtained as stable suspensions in aqueous media by simply introducing phospholipids as the stabilizer.^[28] In one example, lecithin (a mixture of

glycerophospholipids) and 1,2-distearoyl-sn-glycero-3-phosphoethanolamine-N-[methoxy(polyethylene glycol)-5000] (DSPE-PEG) at a weight ratio of 3:1 were employed to stabilize the as-formed PCM nanoparticles. Figure 4A shows a schematic illustration of the resultant PCM nanoparticles, in which the eutectic mixture of lauric and stearic acids, together with an anticancer drug (doxorubicin, DOX) and a NIR dye (IR780), is in direct contact with the hydrophobic aliphatic chains of lecithin and DSPE-PEG. The hydrophilic moieties of lecithin and DSPE-PEG are exposed to the aqueous environment.^[28] The presence of PEG chains in DSPE-PEG was able to markedly increase the stability of the nanoparticles in an aqueous medium.^[47,48] Figure 4B shows a typical TEM image of the PCM nanoparticles, indicating good uniformity and stability. As illustrated in Figure 3, PCM nanoparticles with tunable sizes and stabilized by lecithin and DSPE-PEG could be routinely produced by integrating the anti-solvent-induced precipitation method with a fluidic device.^[46] For this system, it is worth emphasizing that both lecithin and DSPE-PEG, as well as the fatty acids, have all been approved by the Food and Drug Administration (FDA) for clinical applications.

4.2. Substitution into Low-Density Lipoproteins

Similar to the structures self-assembled from phospholipids, many other natural biological materials such as exosomes, lipoproteins, plasma membranes, bacteria, and viruses, have also received considerable attention in serving as carriers for drug delivery.^[59–61] Among them, lipoproteins are perfect candidates for encapsulating PCM made of fatty acids or fatty alcohols, because these structures are produced endogenously for the transportation of lipid molecules in an aqueous environment.^[61–63] Among various types of lipoproteins, low-density lipoproteins (LDLs) are particularly interesting due to their compact sizes (below 50 nm in diameter), high loading capacity, extended circulation time, and low immunogenicity.^[63,64] Each LDL has a well-defined architecture constructed by a shell of amphiphilic phospholipid monolayer embedded with an apolipoprotein known as ApoB-100 and a hydrophobic core composed of more than 45 wt.% cholesteryl esters.^[63–65] The apolipoprotein can be specifically recognized by the LDL receptor, which is up-regulated in many types of malignant cells.^[57,66,67] This unique feature allows LDLs to serve as a class of natural nanoscale carriers for targeted drug delivery.^[63,64] In one report, LDLs were demonstrated to encapsulate PCMs loaded with therapeutic agents.^[57] Typically, the inner cholesteryl esters of LDLs were firstly removed by extraction with heptane. The resultant LDLs were dispersed in a toluene solution containing PCM (the eutectic mixture of lauric and stearic acids), chemotherapeutics, and a NIR dye. The PCM and payloads are naturally driven into the hydrophobic cavity of LDLs through the hydrophobic interaction. After further separation, LDLs loaded with PCM were obtained. Figure 4, C and D, shows a schematic of the structure and TEM image, respectively, of the PCM-substituted LDLs.

4.3. Encapsulation in SiO₂ Hollow Nanoparticles with a Hole in the Wall

As mentioned above, encapsulation of PCM into a solid shell will hinder the loading and release of payloads. To address this problem, hollow nanoparticles with a well-defined hole in the wall have been developed to encapsulate PCMs for temperature-controlled release of therapeutic agents (Figure 5A).^[54] Encapsulation of PCM in such particles can protect them from directly interacting with the biological system, improving their structural stability in

physiological environments. At the same time, the opening allows for fast loading and controlled release of the loaded payloads. In addition, this kind of hollow particles with an opening also ensures a high encapsulation capacity. In this study, the nanoscale capsules were prepared through site-selected deposition by templating with Au-PS Janus colloidal particles.^[54,68,69] Briefly, a hydrophobic precursor, vinyltrimethoxysilane, was used to deposit a shell made of vinyl-silica on the hydrophobic, PS surface only, while exempting the hydrophilic, Au surface. After sequential removal of Au nanoparticles by etching and PS beads by calcination, SiO₂ hollow nanoparticles with a single well-defined hole in the wall were obtained. Figure 5B shows a TEM image of the as-obtained SiO₂ capsules with an average diameter of 192 nm, a wall thickness of 16 nm, and a hole of 24 nm in diameter.

A PCM, together with an anticancer drug and a NIR dye, could be readily loaded into the cavity of the SiO₂ nanocapsule through the hole in the wall (Figure 5A).^[54] Briefly, the capsules were dispersed in a dimethyl sulfoxide solution containing the eutectic mixture of lauric and stearic acids, DOX, and indocyanine green (ICG). Once the cavity of the SiO₂ capsules had been filled with the solution, the particles were collected by centrifugation and water was then added to solidify the fatty acids, with both DOX and ICG trapped inside the PCM. The successful loading of PCM and payloads into the SiO₂ capsules was validated by TEM (Figure 5C) and UV-vis spectroscopy (Figure 5D), respectively. Upon ICG-enabled photothermal heating, the PCM would be melted to undergo a phase transition from solid to liquid, triggering the release of drugs. The amount of the released drug could be controlled by varying the size of the hole and/or the duration of laser irradiation. As another advantage of this system, multiple types of functional materials can be conveniently loaded in large quantities to suit various biomedical applications.^[54,70–72]

4.4. Loading into Mesoporous SiO₂ Nanoparticles

Mesoporous nanoparticles have been extensively used as carriers for various therapeutics. Among them, mesoporous SiO₂ nanoparticles (MSNs) are most popular in biomedical applications due to their biocompatibility and easy production.^[73,74] They have also been demonstrated as carriers to load PCM for stimuli-responsive release of drugs.^[75,76] In one study, MSNs with a maghemite core, *i.e.* γ -Fe₂O₃@MSN core-shell nanoparticles, were used to load PCM (1-tetradecanol) together with therapeutic drugs for controlled release.^[75] The drug molecules were sealed in the mesopores of MSNs with the help of solid PCM. The drug could be released when PCM was melted upon direct heating. The presence of γ -Fe₂O₃ core also offers feasibility for magnetic heating and magnetic resonance imaging (MRI) under magnetic field,^[77,78] and these features are yet to be demonstrated in future studies. Besides MSNs, mesoporous nanoparticles made of Fe₃O₄ or Fe-doped Ta₂O₅ have also been combined with PCM for temperature-regulated release of therapeutic agents.^[79,80]

4.5. Loading into Gold Nanocages

As another class of hollow and porous particles, Au nanocages (AuNCs) can also be used to encapsulate PCM for NIR-triggered release of drugs. First reported by our group in 2002, AuNCs can be conveniently prepared *via* the well-established galvanic replacement between HAuCl₄ and Ag nanocubes.^[81–83] Prompted by their hollow interiors, porous walls, and tunable optical absorption, AuNCs have been explored for an array of applications related to

optical imaging contrast enhancement, photothermal treatment, as well as controlled release and site-specific delivery of drugs.^[84–88] Specifically, the inherent photothermal property of AuNCs makes them immediately useful for triggering the melting of PCM with NIR irradiation. At the same time, the multiple pores in the wall allow for quick loading and release of the payloads. Taken together, a combination of PCM with AuNCs has found extensive use in controlled release.

The first demonstration of encapsulating PCM in AuNCs was reported in 2011.^[10] In that study, AuNCs with an edge length of 60 ± 11 nm and multiple pores (*ca.* 10 nm in size) in the wall (as shown in Figure 5E) were prepared through the galvanic replacement reaction. Rhodamine 6G (R6G) and methylene blue (MB) were used as the mimics of chemotherapeutics and thoroughly mixed with molten 1-tetradecanol (the PCM with a melting point of 38 °C), followed by the introduction of AuNCs. After the mixture of PCM and dye molecules had entered the hollow interiors of the nanocages through the pores, a small amount of hot water was added to induce the phase separation. The AuNCs loaded with PCM and dye were extracted into the water phase owing to their hydrophilic nature. Finally, the AuNCs were collected by centrifugation. The TEM image of the final AuNCs in Figure 5F shows a different contrast relative to pristine AuNCs, demonstrating the successful encapsulation of PCM. The loading of R6G or MB was confirmed using UV-vis spectroscopy (Figure 5G). For this system, either direct heating or irradiation with NIR or high-intensity focused ultrasound (HIFU) could lead to the melting of PCM, resulting in the release of payloads. Later, AuNCs loaded with PCMs have been developed as a versatile platform for the triggered release of various materials, and it can be easily integrated with an array of functions, including imaging, targeted delivery, photothermal therapy, and photodynamic therapy.^[89–92] More examples will be presented in Sections 6.

5. Means for Triggering the Phase Transition

5.1. Direct Heating

PCMs undergo reversible phase transitions in response to temperature changes. To this end, the most straightforward way to trigger the solid-to-liquid transition for controlled release is direct heating (Figure 6A). Direct heating is also the simplest method in the lab for evaluating the controlled release effects associated with PCMs. As for *in vivo* applications, direct heating can be locally applied to the skin through the use of various methods or devices, albeit it is not suitable for the treatment of diseases occurring underneath the skin. On the other hand, it is possible to leverage the temperature increase at disease sites due to the pathological stimulus to trigger the drug release. For example, the microenvironment in a solid tumor is typically 1–2 °C warmer than the healthy tissue.^[93] However, it is difficult to precisely control the release profile by only relying on changes in the internal temperature. In most cases, externally induced quick rise of the local temperature at the targeted site is more useful in triggering and managing the release of a drug.

5.2. Irradiation with NIR Light

NIR light offers immediate advantages in achieving the on-demand release of drugs owing to its non-invasiveness and the remote spatiotemporal controllability. In addition, compared to

lights with other wavelengths, NIR light offers deep penetration into soft tissues because of the reduction in scattering and absorption.^[94] To this end, NIR light has been actively used in various biomedical applications, including imaging, diagnosis, and therapy.^[94–96] It has been demonstrated that NIR light is able to remotely melt PCM particles to trigger the release of drugs by incorporating a NIR dye into the PCM (Figure 6B). In one study, PCM-DOX-IR780-lecithin nanoparticles were prepared by loading IR780 (a NIR dye) and DOX (an anticancer drug) into the PCM matrix during a nanoprecipitation process, with lecithin serving as a stabilizer.^[28] When irradiated with an 808-nm laser at an irradiance of 0.4 W cm⁻², the temperature of the nanoparticle suspension increased from 22 to 43 °C due to the photothermal effect of IR780. If the temperature passes the melting point of the PCM, the encapsulated drugs will be triggered to release quickly (Figure 6C). The NIR-triggered drug release was further validated in A549, a human non-small-cell lung cancer cell line, by monitoring the drug distribution under fluorescence microscopy. As shown in Figure 6D, upon the laser irradiation, the rise in temperature substantially changed the fluorescence pattern of DOX inside the cells from punctate like (as in endo-lysosomes) to diffusive (as in cytosol). A noticeable enrichment of DOX in the nucleus was observed after irradiation for 8 min, with the cell viability being reduced to a level of less than 10%. Encapsulation of PCM in nanostructures with intrinsic absorption in the NIR region allows one to trigger the phase transition without adding a NIR dye. As discussed in Section 4.5, AuNCs could not only serve as a capsule for PCM but also a photothermal agent capable of melting the PCM under NIR irradiation.^[90,91,97] In general, AuNCs have a much better photostability than essentially all organic dyes.^[83,92] For *in vivo* applications, the penetration depth of NIR light is limited to a few inches because of the inevitable scattering and absorption by the tissues, making it difficult to heat the deep sites. In addition, NIR-enabled heating typically requires the presence of a photothermal agent, which may increase the complexity of the PCM-based release system.

5.3. Irradiation with High-Intensity Focused Ultrasound

Ultrasound is widely used in clinics as a non-invasive diagnostic tool to image the inside of a human body. HIFU can concentrate multiple intersecting beams of ultrasound precisely at a focal point, causing the local temperature to quickly increase within seconds and thus resulting in tissue necrosis.^[98] To this end, it has been considered as an attractive strategy for cancer treatment.^[98–100] The local temperature increase at the focal point can also be used for spatiotemporally controlled release of drugs at the targeted site with minimum side effects on the surrounding tissues.^[100–102] It has been demonstrated that the focused ultrasound wave could quickly melt the PCM encapsulated in AuNCs to trigger the release of payloads.^[10] In this case, the payloads were mixed with a PCM such as 1-tetradecanol with a melting point of 38 °C and loaded into the hollow interiors of AuNCs. When exposed to HIFU, the PCM was quickly melted, releasing the trapped payloads into the surrounding medium. The release profiles showed a strong dependence on the power of HIFU, offering an opportunity to control the release dosage on demand. It is worth emphasizing that, unlike NIR light, HIFU-induced temperature rise does not require the presence of AuNCs or other photothermal agents, making it more practical toward clinical applications. However, the propagation of HIFU can be interfered by *in vivo* obstacles such as bone and gas cavity and optimization of the procedure will be necessary.

5.4. Exposure to Magnetic Field

When coupled to magnetic nanoparticles, alternating magnetic field can be used to generate thermal energy, and it has been used for hyperthermia-based therapy and controlled release of drugs.^[103–105] It has also been used to melt PCM with the help of magnetic nanomaterials for remote, site-specific, controlled release.^[79] In this work, the therapeutic agents (DOX or paclitaxel) were mixed with melted 1-tetradecanol (the PCM) and then encapsulated into hollow iron oxide nanoparticles. It was demonstrated that the therapeutics could be released under an alternating magnetic field as the PCM was melted by heating. The release kinetics could be adjusted simply by remotely switching on and off the magnetic field. An *in vivo* study demonstrated that injection of the nanoparticles caused regression for the liver tumor xenograft in nude mice when treated with an alternating magnetic field for 16 days.^[79] Both chemotherapy and hyperthermia contributed to the anti-cancer ability. In addition, the magnetic nanoparticles used in this system can provide additional functions such as targeted delivery and MRI.^[77,78] Similar to NIR light, the generation of heat under alternating magnetic field highly relies on magnetic nanomaterials, which will increase the complexity of the PCM-based release system.

6. Applications

6.1. Protection of Reactive Species

The solid matrix made of a PCM is well-suited for the protection and stabilization of reactive species.^[49,50,90,106] In one study, the concept was demonstrated with 2,2'-azobis[2-(2-imidazolin-2-yl)propane] dihydrochloride (AIPH), a water-soluble azo compound capable of generating alkyl radicals upon decomposition.^[107] The generated radicals can induce apoptosis of cancer cells through DNA damage and peroxidation of proteins and lipids.^[108] However, AIPH is chemically unstable due to its susceptibility to decomposition *in vivo*, which inevitably reduces its availability at the tumor site and increases the side effects. To address this problem, AIPH was mixed with a PCM and encapsulated in the cavities of AuNCs.^[90] Upon irradiation with a NIR laser, the PCM was melted, leading to the release and decomposition of AIPH to generate reactive alkyl radicals. *In vitro* experiment demonstrated that the radicals caused the apoptosis and necrosis of A549 cancer cells. It is worth mentioning that the generation of reactive species from AIPH is oxygen-independent, making this system suitable for cancer treatment under hypoxic conditions, under which the tumor cells are highly resistant to conventional chemotherapy and radiotherapy. In addition to AIPH, other reactive materials such as MnO₂ nanoparticles capable of generating H₂O₂^[49] or diethylenetriamine diazeniumdiolate (NONOate) for producing NO gas^[106] could also be encapsulated in the PCM matrix to avoid their pre-reaction during circulation. Upon released at the targeted site, the MnO₂ nanoparticles would react with protons in the local acidic, aqueous environment to generate H₂O₂ for photodynamic therapy, whereas NONOate could generate NO gas to reverse osteoporosis.

6.2. Controlled Release of Growth Factors

Growth factors are generally proteins that are able to regulate various cellular functions, including proliferation, migration, and differentiation. To this end, they have been widely used in tissue engineering and related applications in combination with scaffolding

materials.^[109,110] In general, there is a high demand for the realization of temporal and spatial controls over the delivery of growth factors in a scaffold for augmenting tissue repair or regeneration.^[110–112] In a recent study, a NIR-responsive system based on PCM was developed for the controlled release of nerve growth factors (NGFs) to promote neurite outgrowth.^[44] In this research, PCM microparticles containing growth factors were fabricated through coaxial electrospinning. The setup is shown in Figure 7A, where the outer solution contains the eutectic mixture of lauric and stearic acids while the inner solution encompasses the payloads. Figure 7B shows an SEM image of the as-obtained PCM microparticles, the interiors of which were filled with ICG and NGF. The particles were placed between two layers of electrospun fibers, generating a scaffold with a sandwich-like structure (Figure 7C). After seeding with spheroids of PC12 cells, the scaffold was irradiated with a diode laser at a power density of 1.0 W cm^{-2} for 6 s and repeated six times at an interval of 2 h. Figure 7D shows a fluorescence micrograph of the spheroids with extending neurites after incubation for seven more days. The greatly extended neurites confirmed that the growth factor could be released under NIR laser, promoting the outgrowth of neurites from spheroids of PC12 cells. This approach based on PCM for controlled release of growth factors should be extendable to release other biomacromolecules such as proteins, RNA, and DNA.

6.3. Encapsulation of Functional Particles

Functional particles can also be encapsulated in the PCM matrix to offer specific features for temperature-controlled release.^[11,37,49] In one study, gelatin particles containing fluorescein isothiocyanate-dextran (FITC-dextran) were encapsulated in PCM for achieving multi-stage release.^[11] The gelatin particles were prepared with diameters in the range of $0.3\text{--}2 \mu\text{m}$ using the emulsification method. Next, these gelatin particles were encapsulated in a PCM (1-tetradecanol or dodecanoic acid) through the use of a fluidic device, where the melted PCM containing gelatin particles serving as the discontinuous phase and an aqueous solution of poly(vinyl alcohol) as the continuous and collection phases. Figure 8A shows a fluorescence micrograph of the resultant 1-tetradecanol particles with a mean diameter of $240 \mu\text{m}$, confirming the successful encapsulation of the FITC-dextran loaded gelatin particles. The confocal fluorescence image in Figure 8B further verified that the FITC-dextran was concentrated in individual gelatin particles. Next, the release profile of FITC-dextran from the PCM particles was measured in water held at $60 \text{ }^\circ\text{C}$. Gradually, as shown in Figure 8C, the fluorescence intensity faded away over time, suggesting their release from the PCM particles. As illustrated in the insets of Figure 8C, it was proposed that upon heating, the PCM melted first, leading to the exposure of gelatin particles to warm water. FITC-dextran was then released due to the dissolution of gelatin. In this type of multi-stage release system, the release profile is mainly determined by the dissolution kinetics of the smaller particles. For example, when three classes of particles made of gelatin, chitosan, and PLGA and loaded with FITC-dextran were encapsulated in PCM, the release rate of FITC-dextran followed the order of gelatin > chitosan > PLGA.^[11] This result was consistent with their solubility in water. In addition to the creation of such a multi-stage release system, encapsulation of functional nanoparticles such as Fe_3O_4 nanoparticles into PCM offers additional features such as targeted delivery and MRI.^[49,77,78]

6.4. Controlled Release of Therapeutics for Cancer Treatment

Chemotherapy is one of the most commonly used methods for cancer treatment. Despite its extensive use and well-documented success, the patients are inevitably burdened with harmful side effects. Since the toxicity of the anticancer drug is dose-dependent, its off-target toxicity can be effectively mitigated by placing a tight control over the instant concentration of drug molecules in the tissue. This aim can be achieved through the development of a system that barely releases the drug unless under an external stimulus.^[4,6,8,113] PCMs are able to perform this function by serving as a smart “gatekeeper” for the therapeutic agents. In the absence of stimuli, the material exists in the solid state to strongly hold the drugs. When the temperature rises under stimuli, the material will be melted to release the drugs. In this case, thermotherapy will occur simultaneously, resulting in a combination effect with chemotherapy. For example, in a recent study, a commercial anticancer drug (DOX) and a NIR dye (IR780) were loaded into PCM nanoparticles for treatment of cancer cells. The loading content of DOX in PCM was about 2.8%. Under NIR laser irradiation, the cells were effectively killed as a result of the quick release of the anticancer drug, as well as the elevation in temperature.^[28] It is worth mentioning that the loading capacity can be improved by switching from hydrophilic DOX to hydrophobic drugs (or pro-drugs) owing to the relatively hydrophobic nature of the PCM.^[57]

Another advantage of PCMs serving as the “gatekeeper” is that they are able to work with multiple types of therapeutics with different properties. Besides commercial anticancer drugs such as DOX, inorganic species such as SeO_3^{2-} and Ca^{2+} can be also easily loaded into PCM matrix and then be delivered to specific sites for killing cancer cells (Figure 9A).^[91,97] It has been demonstrated that SeO_3^{2-} is able to kill cancer cells, even though selenium is an essential element for the development of human body.^[114–116] However, it is a challenge to encapsulate such inorganic ions and deliver them into tumor cells due to their small size and high solubility in aqueous solution. Remarkably, PCM showed the superiority in loading and delivering this kind of inorganic ion.^[91] In one demonstration, H_2SeO_3 and PCM (lauric acid) were dissolved in methanol and then loaded into AuNCs. After removal of the unloaded solution, the PCM was solidified inside AuNCs upon the addition of water, retaining H_2SeO_3 and thus forming AuNC-PCM- H_2SeO_3 nanoparticles. The solid PCM matrix could hold the H_2SeO_3 inside the AuNCs and avoid its dissolution in an aqueous physiological environment. The loading capacity of H_2SeO_3 could be a level as high as 9.2%. Upon NIR laser irradiation, the H_2SeO_3 could be released inside A549 tumor cells, impairing the mitochondrial function (Figure 9, B and C) and finally leading to cell death (Figure 9, D and E). Using a similar method, a large amount of Ca^{2+} ions could be delivered into cells for cancer therapy.^[97] Calcium ions (Ca^{2+}) are important components of tissues and play critical roles in various metabolisms. Normally, the concentration of Ca^{2+} inside cells (*ca.* 0.1 μM) is kept four orders of magnitude lower than the extracellular value (1–10 mM).^[117,118] A marked elevation in the intracellular Ca^{2+} concentration will lead to cell death by damaging intracellular proteins and nucleic acids, as well as organelles such as mitochondria.^[119,120] Leveraging this phenomenon, Ca^{2+} ions were loaded into AuNCs with the help of PCM and quickly released inside cells to kill cancer cells.^[97] *In vitro* analysis suggested that upon laser irradiation, the Ca^{2+} released inside tumor cells effectively destructed the mitochondria and resulted in cell death.

6.5. Targeted Delivery

Modifying the surface of nanoscale carriers with a targeting ligand is an effective strategy for increasing their accumulation in a specific region of interest.^[121] However, it is difficult to directly conjugate targeting moieties to the surface PCM particles due to the relatively low reactivity of their molecules. This issue can be addressed by functionalizing the stabilizer or capsule on the surface with a targeting ligand. In one study, PCM and anticancer drugs (DOX) were loaded into AuNCs, whose surfaces were then functionalized with SV119 for targeted delivery.^[58] SV119 is a synthetic small molecule capable of specific binding to the sigma-2 receptor that is overexpressed on the surface of breast cancer stem cells (CSCs).^[122–125] As such, the AuNCs could be specifically delivered into breast CSCs for the release of a pre-loaded drug upon irradiation with a stimulus. *In vitro* results indicated that the cellular uptake of AuNCs increased proportionally with the coverage density of SV119. Upon heating to a temperature above the melting point of the PCM, the enhanced cellular uptake of the targeting AuNCs led to much greater toxicity relative to that of the non-targeting counterpart.

In another demonstration, LDLs with the tumor-targeting capability were used to encapsulate PCM and DOX.^[57] The LDL receptor is often up-regulated in many types of malignant cells or tissues.^[57,66,67] To this end, LDLs are able to deliver therapeutics specifically into these aberrant cells. *In vitro* studies demonstrated that LDL nanoparticles loaded with PCM and Coumarin 6 were accumulated in A549 lung cancer cells while barely in NIH-3T3 fibroblast cells (Figure 10, A and B).^[57] Furthermore, when the LDL receptors of cells were blocked, the uptake of LDL nanoparticles in both kinds of cells became negligible (Figure 10, C and D), confirming the targeting ability of LDLs. This was further supported by the fact that the LDL nanoparticles loaded with PCM and anti-cancer drugs showed enhanced toxicity toward tumor cells. Additionally, it was demonstrated that LDL nanoparticles loaded with PCM and IR780 could be accumulated in tumor tissues using mice bearing B16-F10 melanoma xenograft (Figure 10, E and F). This system involving both targeted delivery and controlled release can be an effective method for the treatment of various diseases while mitigating the side effects.

6.6. Corking the Opening of Hollow Particles

In addition to its use as a matrix to host payloads, PCM can also be used as a cork to seal the opening in the wall of a hollow particle. For such particles, the hollow interior offers a high loading capacity while the opening in the surface allowed for the easy and quick loading, making them well-suited for the delivery of a variety of functional components, including therapeutic drugs, biomacromolecules, and even nanoparticles.^[71,72,126–128] Sealing the opening with a cork made of PCM can immediately convert these particles into a controlled release system, in which PCM serves as the “on-off” switch. This concept was demonstrated in 2013 with PS hollow particles featuring an open hole in the wall.^[129] The PS hollow particles were prepared through four steps: partial embedding PS beads in poly(4-vinylpyridine) film, swelling PS in a toluene aqueous suspension, rapid freezing them in liquid nitrogen followed by freeze-drying, and finally removal of poly(4-vinylpyridine) film. Upon loading with payloads, the openings on each hollow particle were sealed with a cork made of PCM by following the procedures shown in Figure 11A. Typically, a PCM film

deposited on a silicon wafer was brought into contact with the PS particles supported on a polydimethylsiloxane (PDMS) substrate. Exposure of the samples to ethanol vapor made the PCM soften and movable, sealing the opening under a vacuum. Figure 11, B and C shows SEM and TEM (insets) images of PS hollow particles on PDMS substrate before and after corking with 1-tetradecanol, respectively. Upon heating, the PCM-based cork could be quickly removed, leading to the release of payloads (Figure 11D). The release kinetics could be tailored by using PCMs comprised of a mixture of 1-tetradecanol (with a melting point at 38 °C) and lauric acid (with a melting point at 44 °C) at different ratios. For example, a ratio of 1-tetradecanol to lauric acid at 0.6 resulted in almost entire release of the pre-loaded dye within 30 min of heating at 39 °C, whereas nearly 12 h was required to liberate a similar amount of dye when the ratio was reduced to 0.05 (Figure 11E).^[129] Furthermore, for this system, the release kinetics could be further tuned through the opening size, which was determined by the degree of PS swelling.^[71,129]

7. Summary and Outlook

We have reviewed recent progress in developing a controlled release system based on PCMs for drug delivery and related applications. This controlled release system is simple and versatile effective, in which the payloads encapsulated in a solid PCM only become mobile when the matrix melts into a liquid. Considering the future translation, fatty acids and their derivatives such as fatty alcohols are ideal candidates owing to their natural availability, low toxicity, biodegradability, diversity, and low cost. One can easily obtain a PCM with a melting point near our body temperature by choosing fatty acids/alcohols with different chain lengths or using their eutectic mixtures. To enable their use in practical applications, PCMs made of fatty acids or fatty alcohols have been fabricated into particles with sizes ranging from nano to microscale for delivering various therapeutic agents. They can also be applied as fillings or corks for hollow particles to provide an “on-off” control on the release of payloads. Over the past decade, PCMs have been developed into a versatile platform for the encapsulation and delivery of commercial anticancer drugs (*e.g.*, DOX and paclitaxel), inorganic ions (*e.g.*, SeO_3^{2-} and Ca^{2+}), reactive species (*e.g.*, AIPH and NONOate), biomacromolecules (*e.g.*, NGFs), and even nanoparticles such as those made of gelatin, Fe_3O_4 , and MnO_2 . It has been demonstrated that both direct heating or heating induced by NIR light, HIFU, or magnetic field could be used to trigger the release of payloads on demand. The controlled release is expected to greatly improve the treatment efficiency of the drugs while reducing the side effects. Despite the successes achieved by the PCM-based system, there are still a number of challenges and research interests that need additional attention in the future.

In vivo Performance

Most of the early studies related to PCM-controlled release are for the demonstration of concepts only. Although several of the release systems have been tested *in vivo* in subcutaneous tumor models based on mice, there is still a long way to go before they can be applied to clinical transitions. To this end, more efforts should be devoted to the evaluation of the stability, reactivity, circulation, distribution, and degradation of the PCM nanoparticles in animal models for promoting their future clinical transitions. The performance of a

controlled release system based on a PCM also needs to be further analyzed and improved in the complex biological environments such as an *in vivo* system.

Disease Treatment

In addition, most of the applications have focused on the potential treatment of cancer, with only a few of them on tissue repair or regeneration. As mentioned above, PCMs can be routinely used to load and release various types of molecules or materials with different dimensions and properties, not restricted to anticancer drugs. To this end, it is reasonable to assume that the PCM-based system also holds the promise for the treatment of other life-threatening diseases such as cardiovascular abnormalities, dementia, viral or bacterial infection. In this case, the major change that needs to be made is to replace the therapeutic agents depending on the disease intended to be cured. Of course, the method for triggering the melting of PCM may also need to be optimized depending on where the disease occurs, as well as the heat resistance capability of the surrounding tissues.

Dual-Temperature-Responsive Release System

Sequential releases of two or more payloads to achieve a combined effect has received increased attention in recent years.^[130,131] For example, it has been demonstrated that the release of anticancer drugs followed by small RNA molecules capable of specifically knocking down the expression of the drug resistance gene could improve the therapeutic efficacy.^[132,133] The step-by-step release of multiple drugs can be easily realized using a PCM-based dual or multi-temperature-responsive release system, in which different types of drugs are separately loaded in PCMs with different melting points. In this case, the drug loaded in the PCM with a relatively lower melting point can be released in the early stage upon heating, while the release of another drug from the PCM with a relatively higher melting-point needs to be triggered at a higher temperature. Significantly, the diversity of fatty acids and fatty alcohols offers immediate feasibility for creating such a dual- or multi-temperature-responsive release system. This concept has been demonstrated in a previous report, in which payloads were encapsulated in a system comprised of an outer layer of 1-tetradecanol (with a melting point at 38 °C) and an inner layer of lauric acid (with a melting point at 44 °C).^[11] Upon heating to 39 °C and 44 °C, the 1-tetradecanol and lauric acid layers would be sequentially melted to release the two different payloads.

Temperature-Set Photothermal Therapy

A PCM also has a unique ability to store and release a large amount of heat at a constant temperature set by its melting point. As such, it can be used as a thermal storage material to prevent the temperature of a system from quickly rising or decreasing, facilitating a biomedical treatment process. Taking photothermal therapy as an example, the local temperature of the lesion has to be controlled within a narrow region (typically, 42–45 °C) to avoid damage to the adjacent normal tissues because of quick heat transfer through tissues. However, how to precisely control the temperature during treatment is still difficult to achieve for the currently used approaches based on NIR light, HIFU, or magnetic field and PCM can serve as a heat absorbent for managing the local temperature of the lesion. When the lesion is overheated, the PCM will undergo a solid-to-liquid transition to absorb the heat, preventing the temperature from continuously arising. On the other hand, when the heating

is discontinued, the PCM will release the latent heat through a liquid-to-solid transition, avoiding a quick drop in temperature. As a result, the PCM can keep the local temperature at a level close to the melting point of the PCM for a relatively long period of time, ensuring effective thermotherapy and/or successful release of the drugs while avoiding damage to the adjacent tissues.

Solid-to-Solid or Liquid-to-Gas Phase Transition

In this review, we mainly focused on the solid-to-liquid phase transition of PCMs, in which the vast change in molecular mobility enables one to control the release of a payload. Other types of phase transitions such as solid-to-solid and liquid-to-gas are also worth exploring for biomedical and other applications. For example, the solid-to-solid transition has been explored for solid-state memory and optical-storage applications by leveraging the difference in resistance or reflectivity between the crystalline and amorphous states.^[16] For liquid-to-gas transition, it has been explored as a mechanism for imaging contrast enhancement.^[134] The dramatic expansion in size during the vaporization of acoustic droplets can increase the contrast under ultrasound imaging.^[134,135] Most of the liquid-to-gas PCMs for imaging applications are made of perfluorocarbons (PFCs) due to their relatively low toxicity and boiling points around 37 °C.^[134,136–138] In one study, the authors prepared the PCM droplets made of a mixture of decafluorobutane and octafluoropropane, followed by modifying their surface with folic acid to achieve targeting.^[137,138] The folic acid molecules help deliver the droplets specifically to the tumor site, enhancing the acoustic signals from tumor cells.

In summary, although there are still many obstacles or challenges, we believe that their unparalleled biocompatibility, as well as the ease of use and multiple choices in terms of materials, will bring a bright future to PCMs for controlled release and related applications. We hope that this Progress Report will not only assist researchers in understanding the potential of PCMs as a new platform for controlled release, but also provide some insights for the rational design of their own PCMs.

Acknowledgments

This work was supported in part by startup funds from the Georgia Institute of Technology, grants from the National Institutes of Health (R01 EB020050 and R01 CA138527), and an NIH Director's Pioneer Award (DP1 OD000798). We are grateful to our coworkers and collaborators for their invaluable contributions to this project.

Author Biographies



Jichuan Qiu received his Ph.D. in materials chemistry and physics from Shandong University in 2018 with Prof. Hong Liu. He joined the Xia group at the Georgia Institute of Technology as a visiting graduate student in 2016 and then continued as a postdoctoral

fellow since 2018. His current research interest includes the design and rational synthesis of nanostructured materials for biomedical applications.



Da Huo received his Ph.D. degree in material science and engineering from Nanjing University in 2015 with Prof. Yong Hu. He then worked as a postdoctoral fellow in the Xia group at the Georgia Institute of Technology from 2015 to 2019. He is currently a professor in the School of Pharmacy at Nanjing Medical University. His research is focused on the development of tumor niche-responsive nanomedicines and understanding of how protein corona affects the metabolic behaviors of nanomedicines.



Younan Xia studied at the University of Science and Technology of China (B.S., 1987) and University of Pennsylvania (M.S., 1993) before receiving his Ph.D. from Harvard University in 1996 (with George M. Whitesides). He started as an assistant professor of chemistry at the University of Washington (Seattle) in 1997 and was promoted to associate professor and professor in 2002 and 2004, respectively. He joined the Department of Biomedical Engineering at Washington University in St. Louis in 2007 as the James M. McKelvey Professor. Since 2012, he holds the position of Brock Family Chair and GRA Eminent Scholar in Nanomedicine at the Georgia Institute of Technology.

References

- [1]. Folkman J, Long DM, Rosenbaum R, Science 1966, 154, 148. [PubMed: 5922861]
- [2]. Hoffman AS, J. Control. Release 2008, 132, 153. [PubMed: 18817820]
- [3]. Uhrich KE, Cannizzaro SM, Langer RS, Shakesheff KM, Chem. Rev. 1999, 99, 3181. [PubMed: 11749514]
- [4]. Wang Y, Shim MS, Levinson NS, Sung H-W, Xia Y, Adv. Funct. Mater. 2014, 24, 4206. [PubMed: 25477774]
- [5]. Lu Y, Aimeetti AA, Langer R, Gu Z, Nat. Rev. Mater. 2016, 2, 16075.
- [6]. Mura S, Nicolas J, Couvreur P, Nat. Mater. 2013, 12, 991. [PubMed: 24150417]
- [7]. Kamaly N, Yameen B, Wu J, Farokhzad OC, Chem. Rev. 2016, 116, 2602. [PubMed: 26854975]
- [8]. Hoffman AS, Adv. Drug Deliv. Rev. 2013, 65, 10. [PubMed: 23246762]
- [9]. Hyun DC, Levinson NS, Jeong U, Xia Y, Angew. Chem. Int. Ed. 2014, 53, 3780.
- [10]. Moon GD, Choi S-W, Cai X, Li W, Cho EC, Jeong U, Wang LV, Xia Y, J. Am. Chem. Soc. 2011, 133, 4762. [PubMed: 21401092]
- [11]. Choi S-W, Zhang Y, Xia Y, Angew. Chem. Int. Ed. 2010, 49, 7904.
- [12]. Sharma A, Tyagi VV, Chen CR, Buddhi D, Renew. Sustain. Energy Rev. 2009, 13, 318.
- [13]. Pielichowska K, Pielichowski K, Prog. Mater. Sci. 2014, 65, 67.

- [14]. Sharma RK, Ganesan P, Tyagi VV, Metselaar HSC, Sandaran SC, *Energy Convers. Manage.* 2015, 95, 193.
- [15]. Farid MM, Khudhair AM, Razack SAK, Al-Hallaj S, *Energy Convers. Manage.* 2004, 45, 1597.
- [16]. Wuttig M, Yamada N, *Nat. Mater.* 2007, 6, 824. [PubMed: 17972937]
- [17]. Wang C, Sun Z, Ma L, Su M, *Anal. Chem.* 2011, 83, 2215. [PubMed: 21338061]
- [18]. Ma Z, Hong Y, Zhang M, Su M, *Appl. Phys. Lett.* 2009, 95, 233101.
- [19]. Himran S, Suwono A, Mansoori GA, *Energy Sources* 1994, 16, 117.
- [20]. Yuan Y, Zhang N, Tao W, Cao X, He Y, *Renew. Sustain. Energy Rev.* 2014, 29, 482.
- [21]. Feldman D, Shapiro MM, Banu D, Fuks CJ, *Sol. Energy Mater.* 1989, 18, 201.
- [22]. Geszke-Moritz M, Moritz M, *Mater. Sci. Eng. C* 2016, 68, 982.
- [23]. Mehnert W, Mäder K, *Adv. Drug Deliv. Rev.* 2012, 64, 83.
- [24]. Calder PC, J. Parenter. *Enter. Nutr.* 2015, 39, 18S.
- [25]. Currie E, Schulze A, Zechner R, Walther Tobias C., Farese Robert V., *Cell Metab.* 2013, 18, 153. [PubMed: 23791484]
- [26]. Mashek DG, Coleman RA, *Curr. Opin. Lipidol.* 2006, 17, 274. [PubMed: 16680032]
- [27]. Müller RH, Mäder K, Gohla S, *Eur. J. Pharm. Biopharm.* 2000, 50, 161. [PubMed: 10840199]
- [28]. Zhu C, Huo D, Chen Q, Xue J, Shen S, Xia Y, *Adv. Mater.* 2017, 29, 1703702.
- [29]. Zhao P, Yue Q, He H, Gao B, Wang Y, Li Q, *Appl. Energy* 2014, 115, 483.
- [30]. Zhang H, Sun S, Wang X, Wu D, *Colloids Surf. A* 2011, 389, 104.
- [31]. Zhang H, Wang X, *Colloids Surf. A* 2009, 332, 129.
- [32]. Shah RK, Shum HC, Rowat AC, Lee D, Agresti JJ, Utada AS, Chu L-Y, Kim J-W, Fernandez-Nieves A, Martinez CJ, Weitz DA, *Mater. Today* 2008, 11, 18.
- [33]. Utada AS, Lorenceau E, Link DR, Kaplan PD, Stone HA, Weitz DA, *Science* 2005, 308, 537. [PubMed: 15845850]
- [34]. Chu L-Y, Utada AS, Shah RK, Kim J-W, Weitz DA, *Angew. Chem. Int. Ed.* 2007, 46, 8970.
- [35]. Choi S-W, Zhang Y, Xia Y, *Adv. Funct. Mater.* 2009, 19, 2943. [PubMed: 20191106]
- [36]. Choi S-W, Cheong IW, Kim J-H, Xia Y, *Small* 2009, 5, 454. [PubMed: 19189332]
- [37]. Lone S, Lee HM, Kim GM, Koh W-G, Cheong IW, *Colloids Surf. A* 2013, 422, 61.
- [38]. Utada AS, Fernandez-Nieves A, Stone HA, Weitz DA, *Phys. Rev. Lett.* 2007, 99, 094502. [PubMed: 17931011]
- [39]. Jaworek A, *Powder Technol.* 2007, 176, 18.
- [40]. Xue J, Xie J, Liu W, Xia Y, *Acc. Chem. Res.* 2017, 50, 1976. [PubMed: 28777535]
- [41]. Jayaraman P, Gandhimathi C, Venugopal JR, Becker DL, Ramakrishna S, Srinivasan DK, *Adv. Drug Deliv. Rev.* 2015, 94, 77. [PubMed: 26415888]
- [42]. Xue J, Wu T, Dai Y, Xia Y, *Chem. Rev.* 2019, 119, 5298. [PubMed: 30916938]
- [43]. Trotta M, Cavalli R, Trotta C, Bussano R, Costa L, *Drug Dev. Ind. Pharm* 2010, 36, 431. [PubMed: 19788405]
- [44]. Xue J, Zhu C, Li J, Li H, Xia Y, *Angew. Chem. Int. Ed.* 2018, 28, 1705563.
- [45]. Davoodi P, Feng F, Xu Q, Yan W-C, Tong YW, Srinivasan MP, Sharma VK, Wang C-H, *J. Control. Release* 2015, 205, 70. [PubMed: 25483422]
- [46]. Chen Q, Zhu C, Huo D, Xue J, Cheng H, Guan B, Xia Y, *Nanoscale* 2018, 10, 22312. [PubMed: 30467567]
- [47]. Zhang L, Chan JM, Gu FX, Rhee J-W, Wang AZ, Radovic-Moreno AF, Alexis F, Langer R, Farokhzad OC, *ACS Nano* 2008, 2, 1696. [PubMed: 19206374]
- [48]. Chan JM, Zhang L, Yuet KP, Liao G, Rhee J-W, Langer R, Farokhzad OC, *Biomaterials* 2009, 30, 1627. [PubMed: 19111339]
- [49]. Zhang S, Li Q, Yang N, Shi Y, Ge W, Wang W, Huang W, Song X, Dong X, *Adv. Funct. Mater.* 2019, 29, 1906805.
- [50]. Shi B, Ren N, Gu L, Xu G, Wang R, Zhu T, Zhu Y, Fan C, Zhao C, Tian H, *Angew. Chem. Int. Ed.* 2019, 58, 16826.
- [51]. Zhang S, Wang S, Zhang J, Jiang Y, Ji Q, Zhang Z, Wang Z, *J. Phys. Chem. C* 2013, 117, 23412.

- [52]. Hong Y, Ding S, Wu W, Hu J, Voevodin AA, Gschwender L, Snyder E, Chow L, Su M, ACS Appl. Mater. Interfaces 2010, 2, 1685. [PubMed: 20527779]
- [53]. Geng L, Wang S, Wang T, Luo R, Energy Fuel 2016, 30, 6153.
- [54]. Qiu J, Huo D, Xue J, Zhu G, Liu H, Xia Y, Angew. Chem. Int. Ed. 2019, 58, 10606.
- [55]. Min X, Fang M, Huang Z, Liu Y, Huang Y, Wen R, Qian T, Wu X, Sci. Rep. 2015, 5 12964. [PubMed: 26261089]
- [56]. Tahan Latibari S, Mehrali M, Mehrali M, Indra Mahlia TM, Cornelis Metselaar HS, Energy 2013, 61, 664.
- [57]. Zhu C, Pradhan P, Huo D, Xue J, Shen S, Roy K, Xia Y, Angew. Chem. Int. Ed. 2017, 56, 10399.
- [58]. Sun T, Wang Y, Wang Y, Xu J, Zhao X, Vangveravong S, Mach RH, Xia Y, Adv. Healthc Mater. 2014, 3, 1283. [PubMed: 24677807]
- [59]. Batrakova EV, Kim MS, J. Control. Release 2015, 219, 396. [PubMed: 26241750]
- [60]. Yoo J-W, Irvine DJ, Discher DE, Mitragotri S, Nat. Rev. Drug Discov. 2011, 10, 521. [PubMed: 21720407]
- [61]. Thaxton CS, Rink JS, Naha PC, Cormode DP, Adv. Drug Deliv. Rev. 2016, 106, 116. [PubMed: 27133387]
- [62]. Kuai R, Li D, Chen YE, Moon JJ, Schwendeman A, ACS Nano 2016, 10, 3015. [PubMed: 26889958]
- [63]. Ng KK, Lovell JF, Zheng G, Acc. Chem. Res. 2011, 44, 1105. [PubMed: 21557543]
- [64]. Zhu C, Xia Y, Chem. Soc. Rev. 2017, 46, 7668. [PubMed: 29104991]
- [65]. Gotto AM, Pownall HJ, Havel RJ, Methods Enzymol. 1986, 128, 3. [PubMed: 3523141]
- [66]. Véniant MM, Nielsen LB, Borén J, Young SG, Trends Cardiovasc. Med. 1999, 9, 103. [PubMed: 10578525]
- [67]. Vitols S, Cancer Cells 1991, 3, 488. [PubMed: 1840290]
- [68]. Ohnuma A, Cho EC, Camargo PH, Au L, Ohtani B, Xia Y. J. Am. Chem. Soc. 2009, 131, 1352. [PubMed: 19140763]
- [69]. Qiu J, Xie M, Lyu Z, Gilroy KD, Liu H, Xia Y, Nano Lett. 2019, 19, 6703. [PubMed: 31449753]
- [70]. Li X, Zhou L, Wei Y, El-Toni AM, Zhang F, Zhao D, J. Am. Chem. Soc. 2015, 137, 5903. [PubMed: 25909815]
- [71]. Hyuk Im S, Jeong U, Xia Y, Nat. Mater. 2005, 4, 671. [PubMed: 16086022]
- [72]. Qiu J, Camargo PHC, Jeong U, Xia Y, Acc. Chem. Res. 2019, 52, 3475. [PubMed: 31793763]
- [73]. Li Y, Shi J, Adv. Mater. 2014, 26, 3176. [PubMed: 24687906]
- [74]. Tang F, Li L, Chen D, Adv. Mater. 2012, 24, 1504. [PubMed: 22378538]
- [75]. Liu J, Detrembleur C, De Pauw-Gillet M-C, Mornet S, Elst LV, Laurent S, Jérôme C, Duguet E, J. Mater. Chem. B 2014, 2, 59. [PubMed: 32261299]
- [76]. Liu J, Detrembleur C, De Pauw-Gillet M-C, Mornet S, Jérôme C, Duguet E, Small 2015, 11, 2323. [PubMed: 25580816]
- [77]. Lee N, Yoo D, Ling D, Cho MH, Hyeon T, Cheon J, Chem. Rev. 2015, 115, 10637. [PubMed: 26250431]
- [78]. Lee N, Hyeon T, Chem. Soc. Rev. 2012, 41, 2575. [PubMed: 22138852]
- [79]. Zhang Q, Liu J, Yuan K, Zhang Z, Zhang X, Fang X, Nanotechnology 2017, 28, 405101. [PubMed: 28837053]
- [80]. Feng L, Wang C, Li C, Gai S, He F, Li R, An G, Zhong C, Dai Y, Yang Z, Yang P, Inorg. Chem. 2018, 57, 4864. [PubMed: 29634255]
- [81]. Skrabalak SE, Au L, Li X, Xia Y, Nat. Protoc. 2007, 2, 2182. [PubMed: 17853874]
- [82]. Sun Y, Mayers BT, Xia Y, Nano Lett. 2002, 2, 481.
- [83]. Skrabalak SE, Chen J, Sun Y, Lu X, Au L, Copley CM, Xia Y, Acc. Chem. Res. 2008, 41, 1587. [PubMed: 18570442]
- [84]. Chen J, Wiley B, Li Z-Y, Campbell D, Saeki F, Cang H, Au L, Lee J, Li X, Xia Y, Adv. Mater. 2005, 17, 2255.

- [85]. Chen J, Yang M, Zhang Q, Cho EC, Cobley CM, Kim C, Glaus C, Wang LV, Welch MJ, Xia Y, *Adv. Funct. Mater.* 2010, 20, 3684.
- [86]. Xia Y, Li W, Cobley CM, Chen J, Xia X, Zhang Q, Yang M, Cho EC, Brown PK, *Acc. Chem. Res.* 2011, 44, 914. [PubMed: 21528889]
- [87]. Yavuz MS, Cheng Y, Chen J, Cobley CM, Zhang Q, Rycenga M, Xie J, Kim C, Song KH, Schwartz AG, Wang LV, Xia Y, *Nat. Mater.* 2009, 8, 935. [PubMed: 19881498]
- [88]. Yang M, Wang W, Qiu J, Bai M-Y, Xia Y, *Angew. Chem. Int. Ed.* 2019, 58, 17671.
- [89]. Tian L, Gandra N, Singamaneni S, *ACS Nano* 2013, 7, 4252. [PubMed: 23577650]
- [90]. Shen S, Zhu C, Huo D, Yang M, Xue J, Xia Y, *Angew. Chem. Int. Ed.* 2017, 56, 8801.
- [91]. Cheng H, Huo D, Zhu C, Shen S, Wang W, Li H, Zhu Z, Xia Y, *Biomaterials* 2018, 178, 517. [PubMed: 29631784]
- [92]. Chen J, Wang D, Xi J, Au L, Siekkinen A, Warsen A, Li Z-Y, Zhang H, Xia Y, Li X, *Nano Lett.* 2007, 7, 1318. [PubMed: 17430005]
- [93]. Fukumura D, Jain RK, *J. Cell. Biochem.* 2007, 101, 937. [PubMed: 17171643]
- [94]. Weissleder R, *Nat. Biotechnol.* 2001, 19, 316. [PubMed: 11283581]
- [95]. Fomina N, McFearin C, Sermsakdi M, Edigin O, Almutairi A, *J. Am. Chem. Soc.* 2010, 132, 9540. [PubMed: 20568765]
- [96]. Shanmugam V, Selvakumar S, Yeh C-S, *Chem. Soc. Rev.* 2014, 43, 6254. [PubMed: 24811160]
- [97]. Chen Q, Huo D, Cheng H, Lyu Z, Zhu C, Guan B, Xia Y, *Adv. Healthc. Mater.* 2019, 8 1801113.
- [98]. Kennedy JE, *Nat. Rev. Cancer* 2005, 5, 321. [PubMed: 15776004]
- [99]. Fan W, Yung B, Huang P, Chen X, *Chem. Rev.* 2017, 117, 13566. [PubMed: 29048884]
- [100]. Chen Y, Chen H, Shi J, *Adv. Healthc. Mater.* 2015, 4, 158. [PubMed: 24898413]
- [101]. Li W, Cai X, Kim C, Sun G, Zhang Y, Deng R, Yang M, Chen J, Achilefu S, Wang LV, Xia Y, *Nanoscale* 2011, 3, 1724. [PubMed: 21321760]
- [102]. Grüll H, Langereis S, *J. Control. Release* 2012, 161, 317. [PubMed: 22565055]
- [103]. Lee J-H, Jang J-T, Choi J-S, Moon SH, Noh S-H, Kim J-W, Kim J-G, Kim I-S, Park KI, Cheon J, *Nat. Nanotechnol.* 2011, 6, 418. [PubMed: 21706024]
- [104]. Thiesen B, Jordan A, *Int. J. Hyperth.* 2008, 24, 467.
- [105]. Kumar CSSR, Mohammad F, *Adv. Drug Deliv. Rev.* 2011, 63, 789. [PubMed: 21447363]
- [106]. Lin Y-J, Chen C-C, Chi N-W, Nguyen T, Lu H-Y, Nguyen D, Lai P-L, Sung H-W, *Adv. Mater.* 2018, 30 1705605.
- [107]. Yoshida Y, Itoh N, Saito Y, Hayakawa M, Niki E, *Free Radic. Res.* 2004, 38, 375. [PubMed: 15190934]
- [108]. Krishna MC, Dewhirst MW, Friedman HS, Cook JA, Degraff W, Samuni A, Russo A, Mitchell JB, *Int. J. Hyperth.* 1994, 10, 271.
- [109]. Khademhosseini A, Langer R, *Nat. Protoc.* 2016, 11, 1775. [PubMed: 27583639]
- [110]. Tayalia P, Mooney DJ, *Adv. Mater.* 2009, 21, 3269. [PubMed: 20882497]
- [111]. Li J, Linderman SW, Zhu C, Liu H, Thomopoulos S, Xia Y, *Adv. Mater.* 2016, 28, 4620. [PubMed: 27059654]
- [112]. Brudno Y, Mooney DJ, *J. Control. Release* 2015, 219, 8. [PubMed: 26374941]
- [113]. Sun T, Zhang YS, Pang B, Hyun DC, Yang M, Xia Y, *Angew. Chem. Int. Ed.* 2014 53, 12320.
- [114]. Weekley CM, Harris HH, *Chem. Soc. Rev.* 2013, 42, 8870. [PubMed: 24030774]
- [115]. Weekley CM, Aitken JB, Vogt S, Finney LA, Paterson DJ, de Jonge MD, Howard DL, Witting PK, Musgrave IF, Harris HH, *J. Am. Chem. Soc.* 2011, 133, 18272. [PubMed: 21957893]
- [116]. Olm E, Fernandes AP, Hebert C, Rundlöf A-K, Larsen EH, Danielsson O, Björnstedt M, *Proc. Natl. Acad. Sci. U.S.A.* 2009, 106, 11400. [PubMed: 19549867]
- [117]. Campbell AK, *Intracellular calcium, its universal role as regulator*, John Wiley & Sons, Chichester, West Sussex, UK 1983.
- [118]. Carafoli E, *Annu. Rev. Biochem.* 1987, 56, 395. [PubMed: 3304139]
- [119]. Orrenius S, Zhivotovsky B, Nicotera P, *Nat. Rev. Mol. Cell Biol.* 2003, 4, 552. [PubMed: 12838338]

- [120]. Whitfield JF, Bird RP, Chakravarthy BR, Isaacs RJ, Morley P, J. Cell. Biochem. 1995, 59, 74.
- [121]. Wang Y, Brown P, Xia Y, Nat. Mater. 2011, 10, 482. [PubMed: 21685899]
- [122]. Wang Y, Xu J, Xia X, Yang M, Vangveravong S, Chen J, Mach RH, Xia Y, Nanoscale 2012, 4, 421. [PubMed: 22113350]
- [123]. Kashiwagi H, McDunn JE, Simon PO, Goedegebuure PS, Xu J, Jones L, Chang K, Johnston F, Trinkaus K, Hotchkiss RS, Mach RH, Hawkins WG, Mol. Cancer 2007, 6, 48. [PubMed: 17631687]
- [124]. Nakagawa O, Ming X, Huang L, Juliano RL, J. Am. Chem. Soc. 2010, 132, 8848. [PubMed: 20550198]
- [125]. Kashiwagi H, McDunn JE, Simon PO, Goedegebuure PS, Vangveravong S, Chang K, Hotchkiss RS, Mach RH, Hawkins WG, J. Transl. Med. 2009, 7, 24. [PubMed: 19323815]
- [126]. Bai M-Y, Moran CH, Zhang L, Liu C, Zhang Y, Wang LV, Xia Y, Adv. Funct. Mater. 2012 22, 764. [PubMed: 31866803]
- [127]. Jeong U, Im SH, Camargo PHC, Kim JH, Xia Y, Langmuir 2007, 23, 10968. [PubMed: 17910489]
- [128]. Si Y, Chen M, Wu L, Chem. Soc. Rev. 2016, 45, 690. [PubMed: 26658638]
- [129]. Hyun DC, Lu P, Choi S-I, Jeong U, Xia Y, Angew. Chem. Int. Ed. 2013, 52, 10468.
- [130]. Shim G, Kim M-G, Kim D, Park JY, Oh Y-K, Adv. Drug Deliv. Rev. 2017, 115, 57. [PubMed: 28412324]
- [131]. Ong W, Pinese C, Chew SY, Adv. Drug Deliv. Rev. 2019, 149–150, 19.
- [132]. Fan L, Zhang Y, Wang F, Yang Q, Tan J, Grifantini R, Wu H, Song C, Jin B, Biomaterials 2016, 76, 399. [PubMed: 26561936]
- [133]. Ren Y, Wang R, Gao L, Li K, Zhou X, Guo H, Liu C, Han D, Tian J, Ye Q, Hu YT, Sun D, Yuan X, Zhang N, J. Control. Release 2016, 228, 74. [PubMed: 26956593]
- [134]. Huang Y, Vezeridis AM, Wang J, Wang Z, Thompson M, Mattrey RF, Gianneschi NC, J. Am. Chem. Soc. 2017, 139, 15. [PubMed: 28032757]
- [135]. Cox B, Beard P, Nature 2015, 527, 451. [PubMed: 26607538]
- [136]. Rapoport N, Nam K-H, Gupta R, Gao Z, Mohan P, Payne A, Todd N, Liu X, Kim T, Shea J, Scaife C, Parker DL, Jeong E-K, Kennedy AM, J. Control. Release 2011, 153, 4. [PubMed: 21277919]
- [137]. Marshalek JP, Sheeran PS, Ingram P, Dayton PA, Witte RS, Matsunaga TO, J. Control. Release 2016, 243, 69. [PubMed: 27686582]
- [138]. Hadinger KP, Marshalek JP, Sheeran PS, Dayton PA, Matsunaga TO, Ultrasound Med. Biol. 2018, 44, 2728. [PubMed: 30228045]

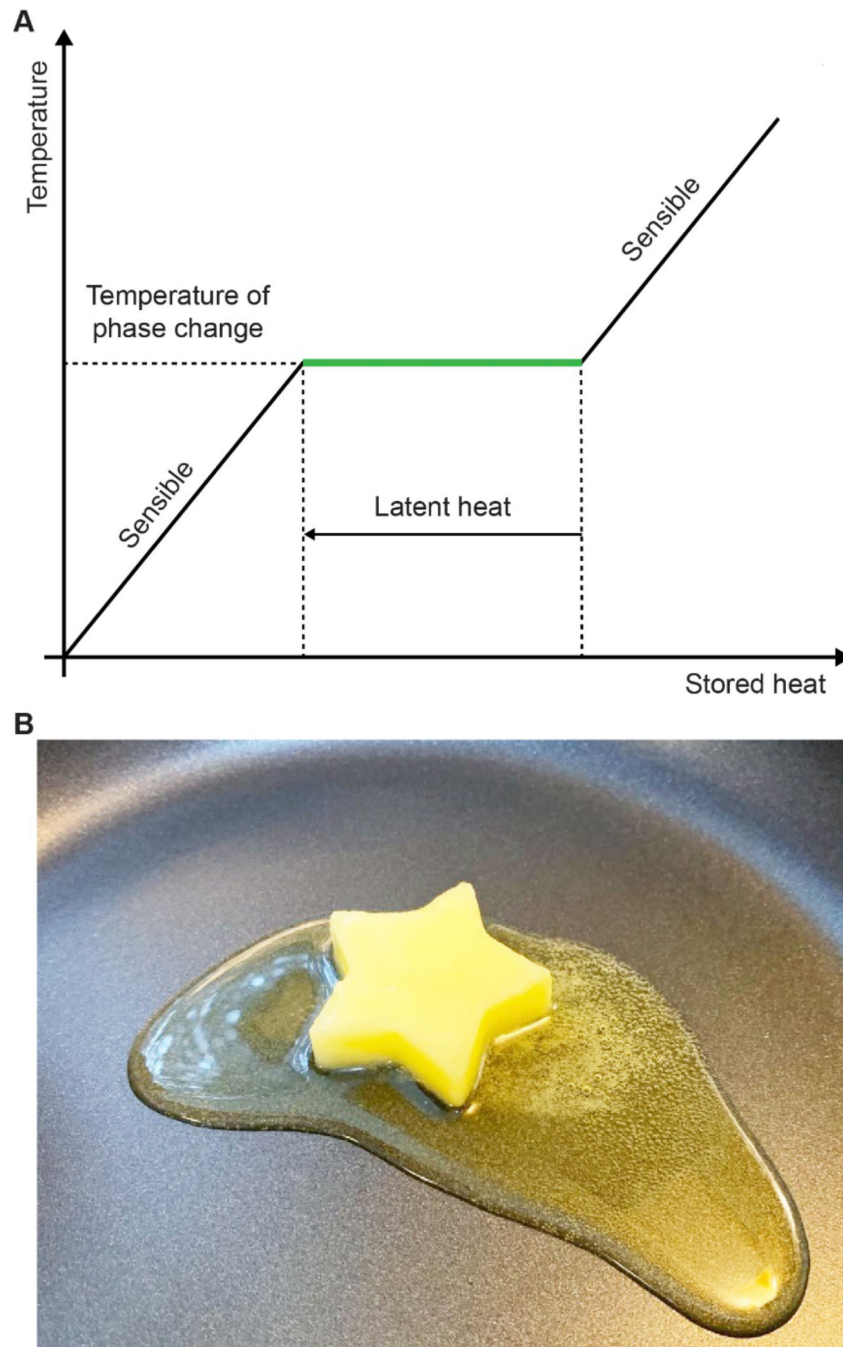


Figure 1. Properties of PCM. (A) A representative phase diagram showing the temperature of a PCM as a function of the stored heat. (B) A digital photograph of a solid butter undergoing melting in a pan, illustrating the drastic increase in molecular mobility during solid-to-liquid transition.

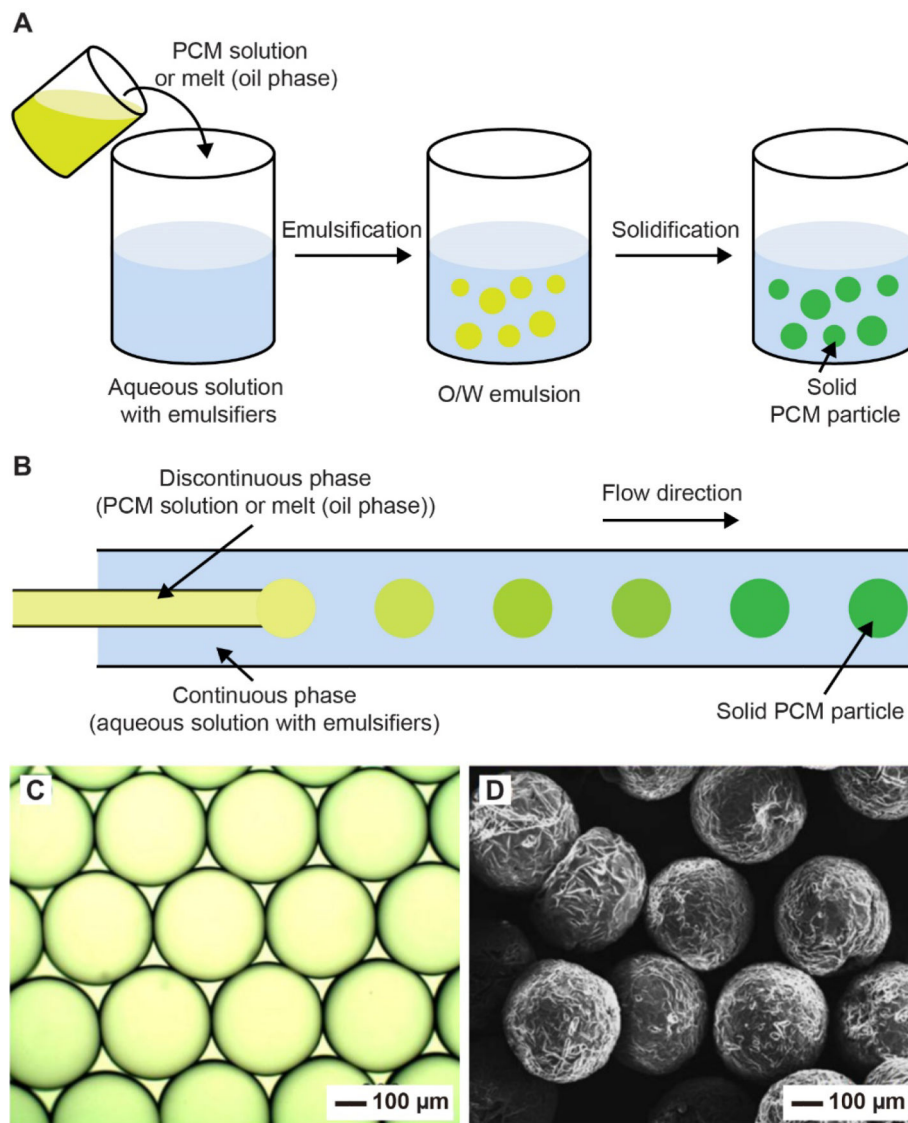


Figure 2. Preparation of PCM particles. (A) Schematic illustration of the three major steps involved in the fabrication of PCM particles through emulsification under shear force: *i*) introduction of PCM melt or solution (oil phase) into an aqueous solution containing appropriate emulsifiers, *ii*) formation of an oil in water (O/W) emulsion under agitation, and *iii*) solidification of the O/W droplets through cooling of the melt or evaporation of the oil phase solvent. (B) Schematic illustration of a fluidic device for the fabrication of uniform PCM particles. (C) Optical micrograph of PCM droplets produced through the fluidic device. (D) SEM image of the solid PCM particles. (B-D) Reproduced with permission.^[37] Copyright 2013, Elsevier.

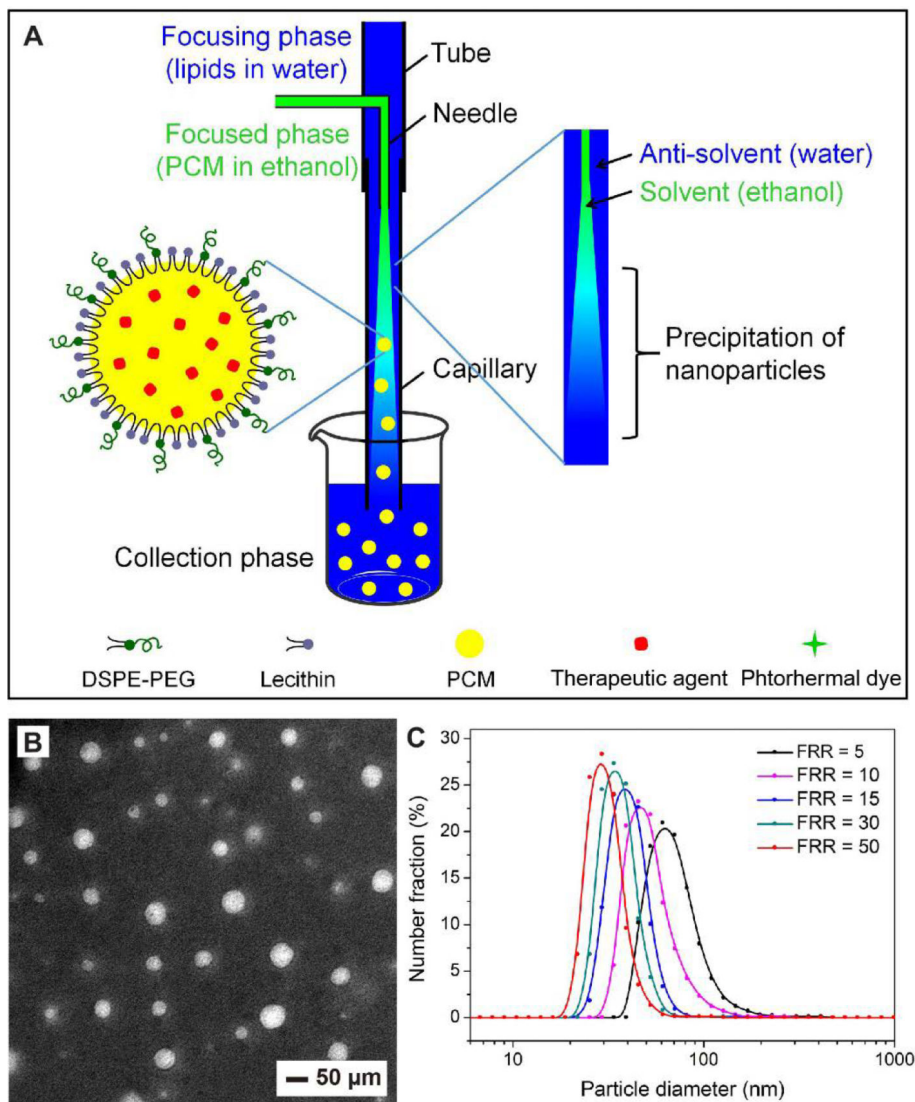


Figure 3. Preparation of PCM nanoparticles through anti-solvent-induced precipitation in a fluidic device. (A) Schematic illustration of the fluidic device used for producing PCM nanoparticles. As the ethanol solution of PCM and an aqueous solution meet and mix along the flow, the PCM precipitates out as nanoparticles at the interface between the focusing and focused phases. Phospholipids are typically used to stabilize the nanoparticles. Therapeutic agents and photothermal dyes can be easily loaded into the PCM nanoparticles by dissolving them in the PCM solution. (B) TEM image of the as-prepared PCM nanoparticles. (C) Size distribution of the PCM nanoparticles prepared at different flow rate ratios (FRRs) between the focusing and focused phases. Reproduced with permission.^[46] Copyright 2017, Royal Society of Chemistry.

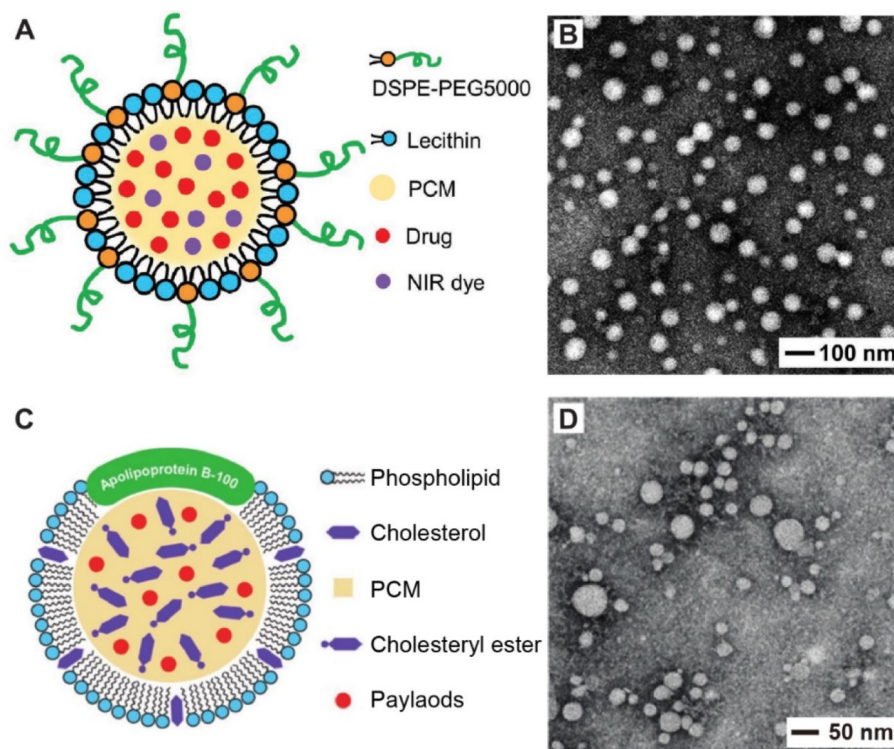


Figure 4. Encapsulation of PCM in phospholipid shells. (A) Schematic illustration of a PCM-DOX-IR780-Lecithin nanoparticle, which was prepared by covering the surface of nanoparticles consisting of PCM, DOX, and IR-780 with a monolayer of soybean lecithin and DSPE-PEG. (B) TEM image of the PCM-IR780-DOX-Lecithin nanoparticles. (C) Schematic illustration of an LDL nanoparticle whose core has been partially replaced with a mixture of PCM and drugs. (D) TEM image of the LDL nanoparticles containing a mixture of PCM and drugs. (A, B) Reproduced with permission.^[28] Copyright 2017, Wiley-VCH. (C, D) Adapted with permission.^[57] Copyright 2017, Wiley-VCH.

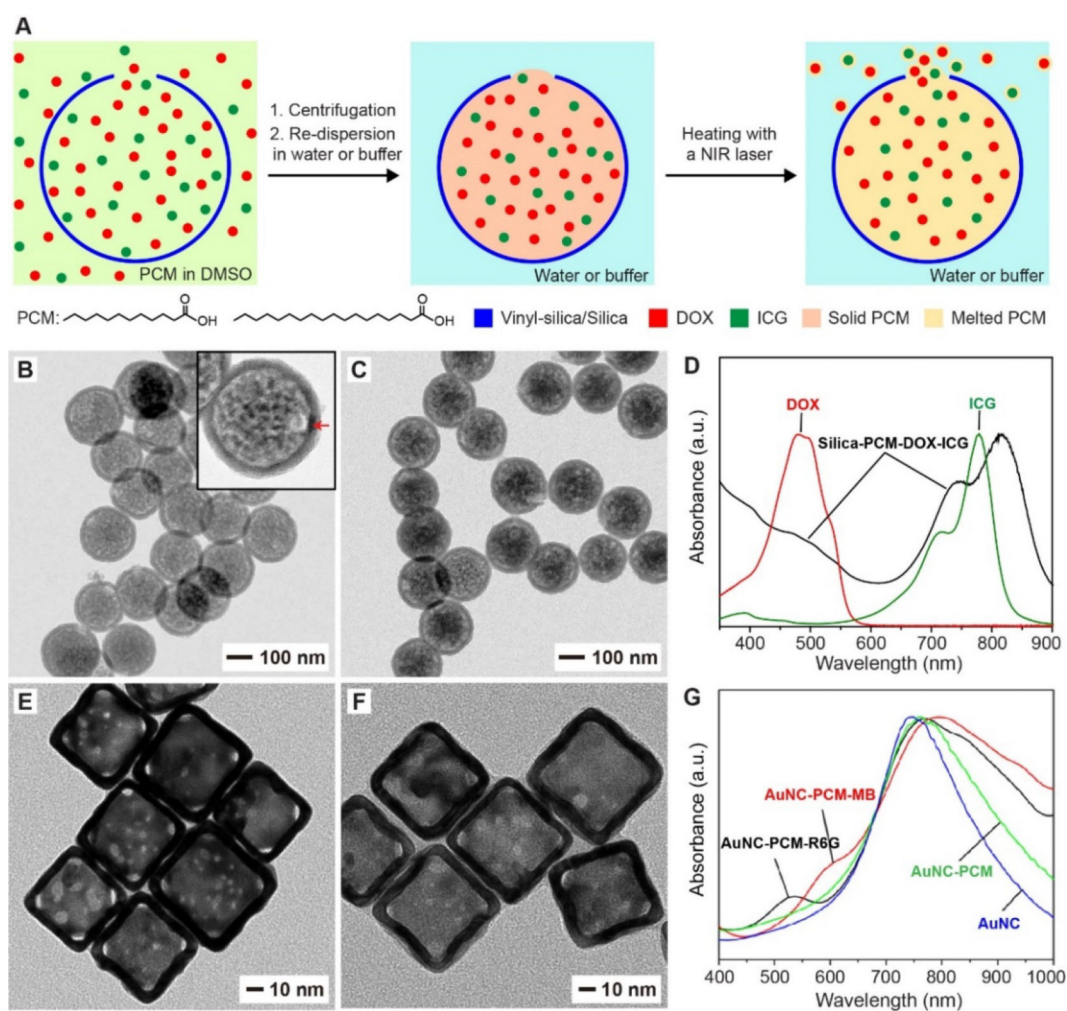


Figure 5. Encapsulation of PCM in hollow nanoparticles with one or multiple holes in the wall. (A) Schematic illustration showing the encapsulation and release of PCM, anticancer drug (DOX) and NIR dye (ICG) in silica hollow nanoparticles with one hole in the wall. (B, C) TEM images of silica nanoparticles (B) before and (C) after loading with PCM and payloads. The success of loading PCM into the nanoparticles is manifested by the changes in contrast. (D) UV-vis spectrum of the resultant nanoparticles, confirming the successful loading of both DOX and ICG. (E, F) TEM images of AuNCs (E) before and (F) after loading with PCM and payloads. (G) UV-vis spectra of the resultant AuNCs, confirming the successful loading of R6G or MB. (A-D) Reproduced with permission.^[54] Copyright 2019, Wiley-VCH. (E-G) Adapted with permission.^[10] Copyright 2011, American Chemical Society.

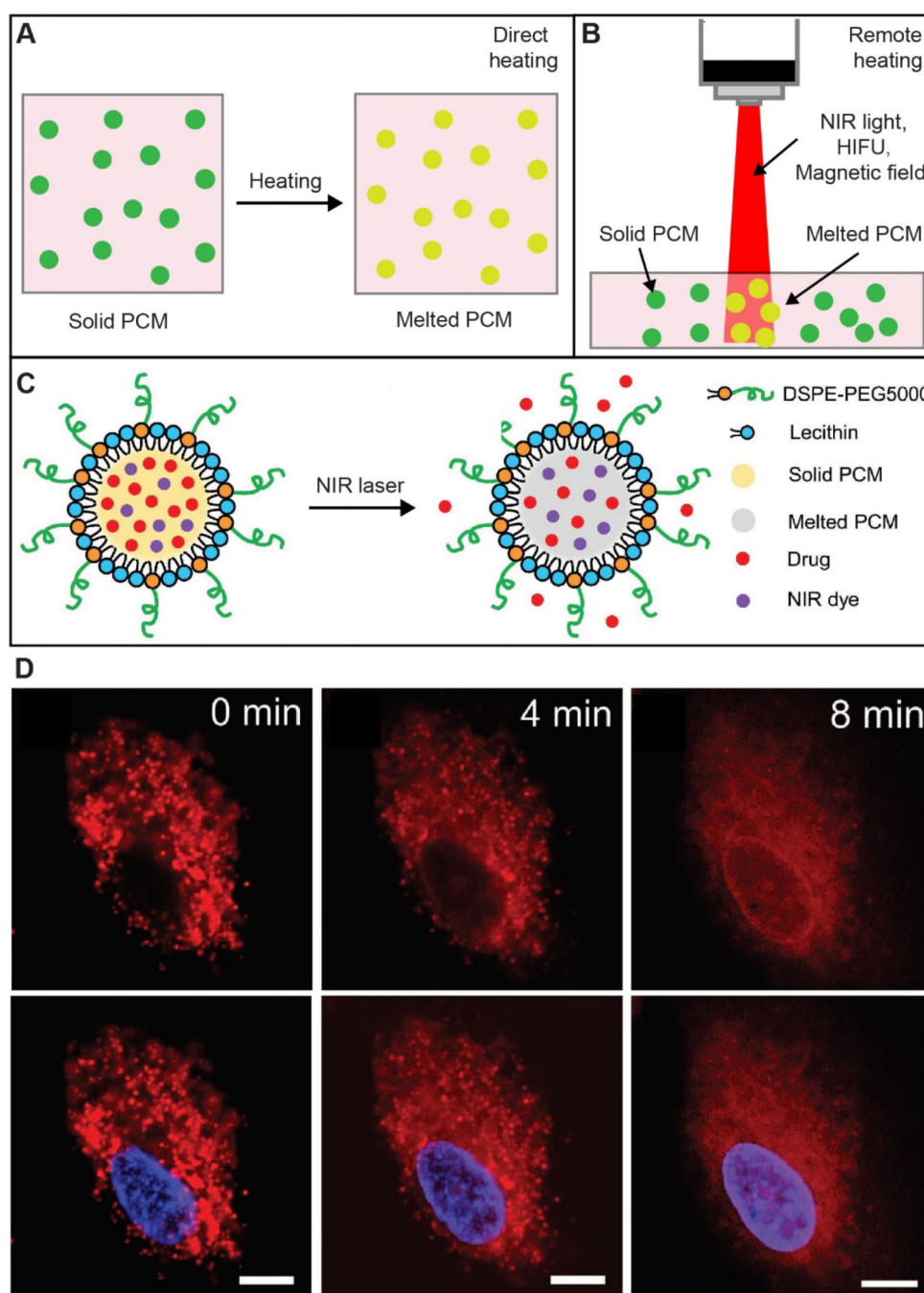


Figure 6. Means for triggering the phase transition of PCM. (A, B) Schematic illustrations showing the phase transition of PCM particles through (A) direct heating and (B) heating induced by NIR light/HIFU/magnetic field. (C) Schematic illustration of NIR-triggered release of drugs from a PCM-DOX-IR780-lecithin nanoparticle. (D) Time-course DOX (red) release from the PCM-DOX-IR780-lecithin nanoparticles in a human non-small cell lung cancer cell (A549) upon irradiation with an 808-nm laser (power density: 0.2 W cm^{-2}). The nucleus

was stained blue by Hoechst 33342. Scale bars: 10 μm . (C, D) Reproduced with permission.
[28] Copyright 2017, Wiley-VCH.

Author Manuscript

Author Manuscript

Author Manuscript

Author Manuscript

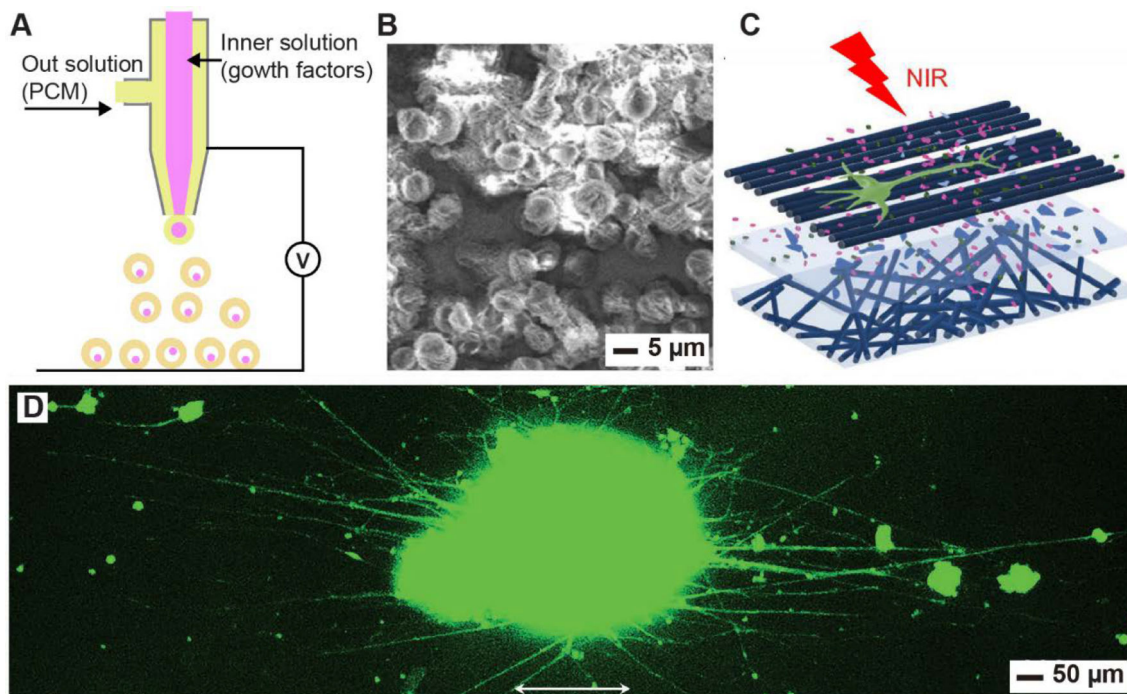


Figure 7. Encapsulation and controlled release of growth factors for tissue engineering. (A) Schematic illustration of a coaxial electrospay setup for the preparation of PCM microparticles containing NGFs and NIR dyes in the core. (B) SEM image of the as-obtained PCM microparticles. (C) Schematic illustration showing the outgrowth of neurites from spheroids of PC12 cells in a sandwich-like scaffold when NGFs were released from the PCM microparticles under the irradiation with an 808-nm laser. (D) Fluorescence image of the typical neurite fields extending from the spheroids after NIR-triggered release of NGFs from PCM particles. The neurites were stained with Tuj1 marker (green). The arrows indicate the alignment directions of the fibers. Reproduced with permission.^[44] Copyright 2018, Wiley-VCH.

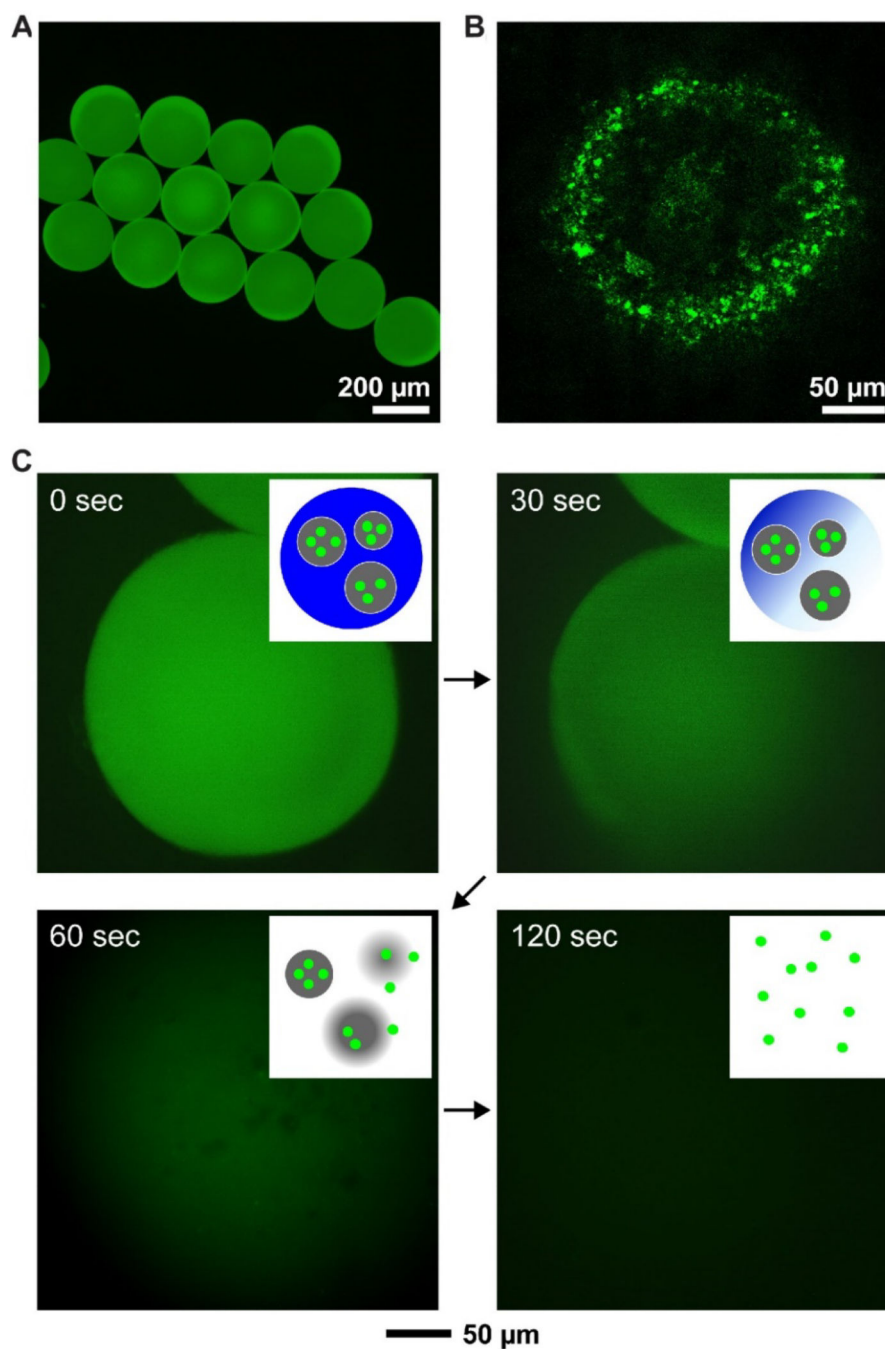


Figure 8. Encapsulation and controlled release of gelatin microparticles. (A) Fluorescence and (B) confocal fluorescence images of uniform PCM beads loaded with gelatin microparticles. The gelatin microparticles were pre-loaded with FITC-dextran molecules. (C) Time-lapse fluorescence analysis showing the release of FITC-dextran from the gelatin microparticles upon the melting of PCM. The insets are schematics illustrating the major steps involved in the release of FITC-dextran. Reproduced with permission.^[11] Copyright 2010, Wiley-VCH.

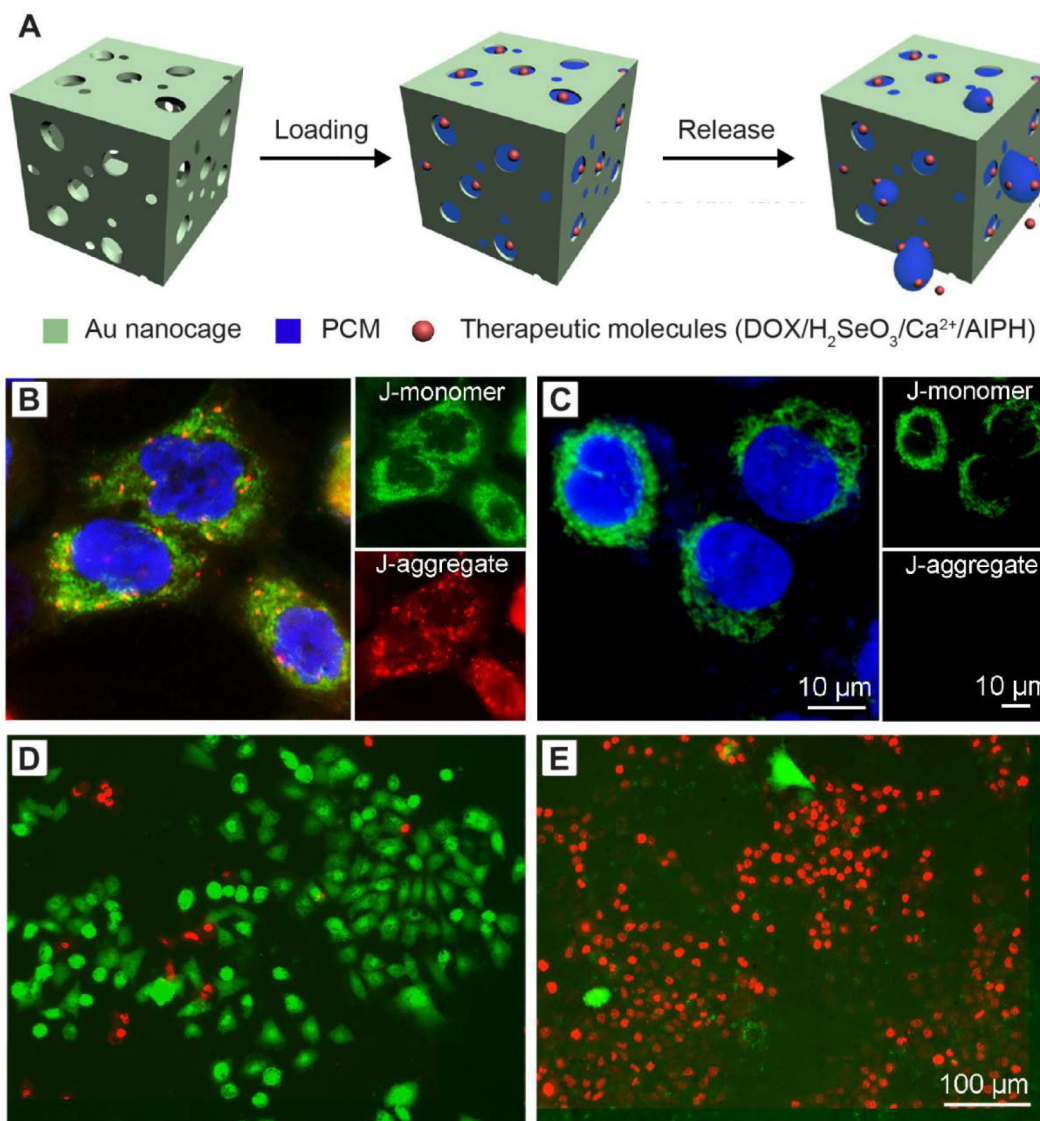


Figure 9.

Encapsulation and controlled release of therapeutic molecules. (A) Schematic illustration showing the encapsulation of PCM and payloads in AuNCs and the subsequent controlled release. The payloads can be DOX, H₂SeO₃, Ca²⁺, or AIPH. (B, C) 5,5',6,6'-tetrachloro-1,1',3,3'-tetraethylimidacarbocyanine iodide staining and (D, E) Live/dead staining of A549 cells after incubation with AuNC-PCM-H₂SeO₃ nanoparticles for 5 h. The cells in (C, E) were further irradiated with an 808-nm laser at a power density of 0.8 W cm⁻² for 10 min before the staining. The red and green fluorescence colors in (B, C) indicate the preservation and loss of mitochondrial membrane potential, respectively. The nuclei were stained to give a blue color. The red and green fluorescence colors in (D, E) indicate the live and dead cells, respectively, which were stained with calcein-AM and ethidiumhomodimer-1. Reproduced with permission.^[91] Copyright 2018, Elsevier.

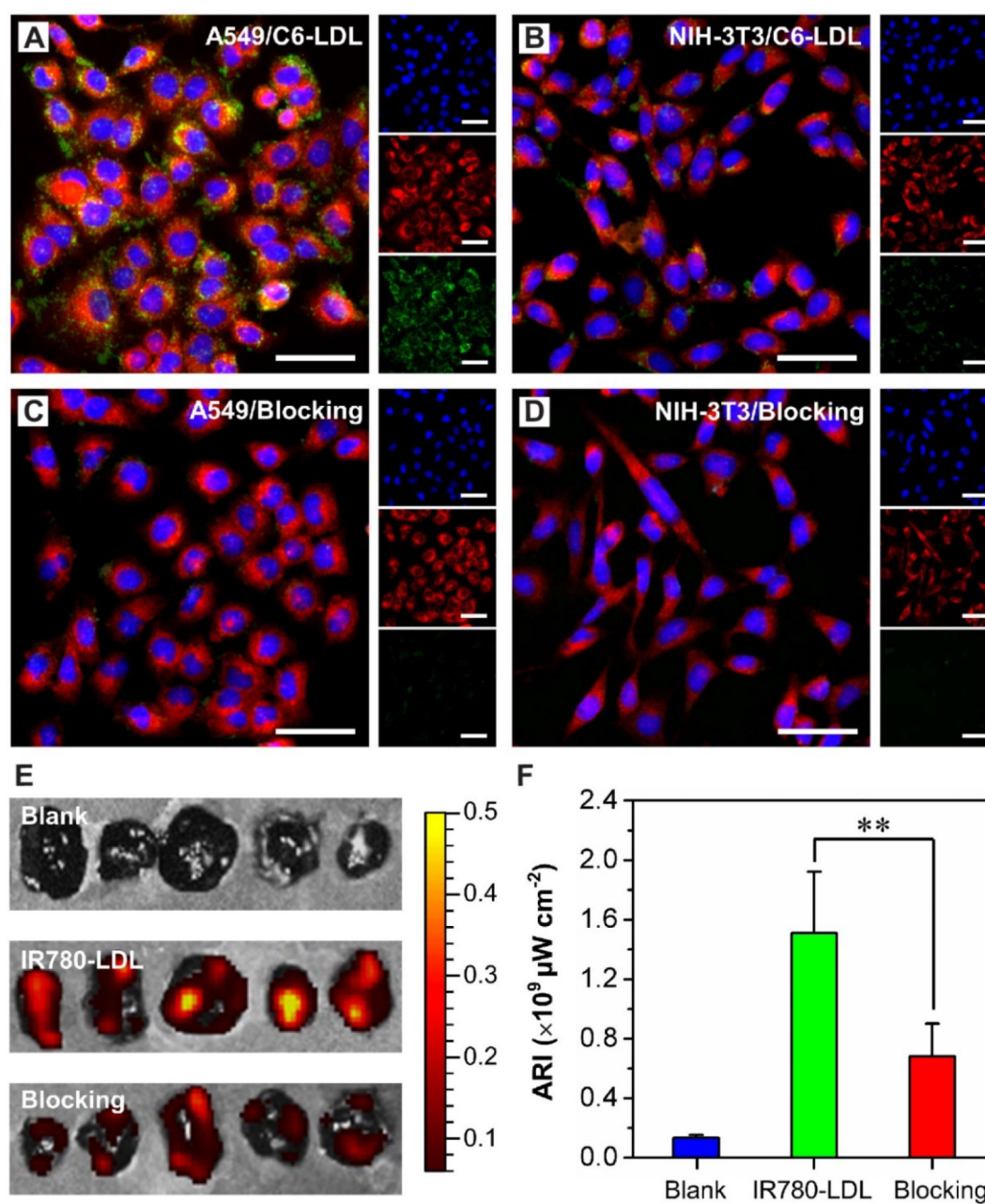


Figure 10.

Selective delivery of PCM nanoparticles. (A-D) The uptakes of LDL nanoparticles loaded with PCM and coumarin 6 by (A, C) A549 and (B, D) NIH-3T3 cells. The receptors of cells in (C) and (D) were blocked with a 20-fold excess of native LDLs. The nuclei were stained blue with Hoechst 33342; the lysosomes were stained red with LysoTracker; coumarin 6 is shown in green. Scale bars: 50 μm . (E, F) In vivo evaluation of the accumulation of LDL nanoparticles in B16-F10 melanoma. (E) Fluorescence images of the tumors excised at 24 h post intravenous injection and (F) the corresponding average radiant efficiency. “Blank”, “IR780-LDL”, and “Blocking” indicate the LDLs loaded with PCM alone, the LDLs loaded with both PCM and IR780, and a mixture of LDLs loaded with PCM and IR780 and 20-fold

excess of native LDLs, respectively. The color bar in (E) represents the radiant efficiency ($\times 10^9 \mu\text{W cm}^{-2}$). Significant difference between the tumors with or without receptor blocking is indicated as $**p < 0.005$. Reproduced with permission.^[57] Copyright 2017, Wiley-VCH.

Author Manuscript

Author Manuscript

Author Manuscript

Author Manuscript

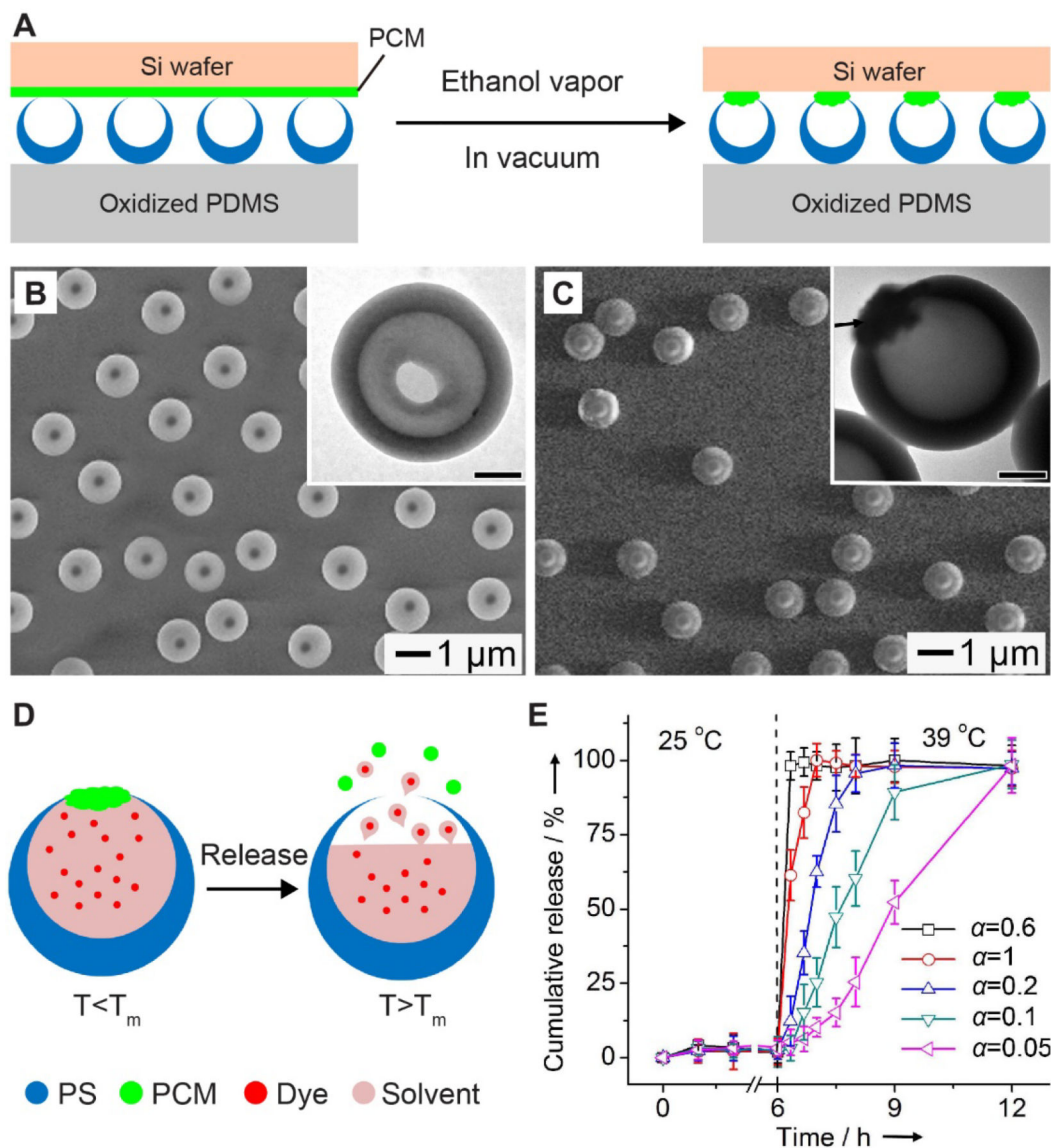


Figure 11.

Corking the opening of hollow particles. (A) Schematic illustration showing the process of corking the openings of PS hollow particles with PCM. (B, C) SEM images of PS hollow particles (B) before and (C) after corking with PCM. The insets are the corresponding TEM images (scale bars: 300 nm). (D) Schematic illustration showing PCM serving as the cork of a PS hollow particle for controlled release of payloads in response to temperature rise. T_m stands for the melting temperature of PCM. (E) Release profiles of the payloads from the particles corked with a binary mixture of PCM made with 1-tetradecanol and lauric acid. The volumetric ratio (α) of 1-tetradecanol to lauric acid was tuned from 0.05:1 to 1:1, which could result in the changes of the melting temperature of the PCM. The scale bars in the insets are 300 nm. Reproduced with permission.^[129] Copyright 2013, Wiley-VCH.

Table 1.A list of fatty acids and fatty alcohols suitable for biomedical applications.^[9,20]

Category	Compound	Number of carbon atoms	Melting point [°C]
Fatty acid	Decanoic acid	10	32
	Lauric acid	12	44
	Myristic acid	14	54.4
	Palmitic acid	16	63
	Stearic acid	18	69
	Linolelaidic acid ^[a]	18	28–29
	Vaccenic acid ^[a]	18	44
	Elaidic acid ^[a]	18	45
	Arachidic acid	20	75.5
	Behenic acid	22	80.0
Fatty alcohol	Dodecanol	12	24
	1-Tridecanol	13	32
	1-Tetradecanol	14	38
	1-Pentadecanol	15	41–44
	Hexadecanol	16	49
	1-Octadecanol	18	59–60

^[a]Unsaturated fatty acids

Table 2.

A list of representative strategies effective in stabilizing PCM colloidal particles and their influence on the loading and release of payloads.

Strategies	Materials involved	Advantages	Disadvantages	Ref.
Coating with a shell of a solid material	SiO ₂ or PS	Easy to apply Significantly improving colloidal stability	Non-degradable <i>in vivo</i> Blocking the loading and release of payloads	[51–53]
Covering with a monolayer of phospholipids	Phospholipids	Easy to apply Biocompatible Biodegradable	Pre-leakage of payloads	[28, 46]
Substitution into LDLs	LDLs	Natural biological materials Biocompatible Biodegradable Targeting capability	Multiple procedures for loading the payloads Limited supply of LDLs	[57]
Encapsulation into hollow particles with an opening	SiO ₂	Easy loading through the opening High loading capacity Suitable for multiple types of payloads Regulation of release	Non-degradable <i>in vivo</i> Multiple procedures for the preparation of the SiO ₂ hollow particles with a hole	[54]
Loading into Mesoporous particles	SiO ₂ or Fe ₃ O ₄ or Fe-doped Ta ₂ O ₅	Easy loading Relatively high loading capacity	Non-degradable <i>in vivo</i> Pre-leakage of payloads	[75, 79, 80]
Loading into AuNCs	Au	Easy loading High loading capacity Suitable for multiple types of payloads Regulation of release Intrinsic photothermal property	Non-degradable <i>in vivo</i> Multiple procedures for the preparation of the AuNCs	[10, 89–92]

PS, polystyrene; LDLs, low-density lipoproteins; AuNCs, gold nanocages